Altered hierarchical auditory predictive processing after lesions to the orbitofrontal cortex

Olgerta Asko,[1,2] Alejandro O. Blenkmann,[1,2] Sabine L. Leske,[2,3] Maja Dyhre Foldal,[1,2] Anaïs Llorens,[4] Ingrid Funderud,[5,6] Torstein R. Meling[7,8], Robert T. Knight,[4] Tor Endestad[1,2,5] and Anne-Kristin Solbakk[1,2,5,7]

Author affiliations:

1 Department of Psychology, University of Oslo, 0373 Oslo, Norway

2 RITMO Centre for Interdisciplinary Studies in Rhythm, Time and Motion, University of Oslo, 0373 Oslo, Norway

3 Department of Musicology, University of Oslo, 0373 Oslo, Norway

4 Helen Wills Neuroscience Institute and Department of Psychology, University of California, Berkeley, CA 947200, USA

5 Department of Neuropsychology, Helgeland Hospital, 8657 Mosjøen, Norway

6 Regional Department of Eating Disorders, Oslo University Hospital, Ullevål, 0450 Oslo, Norway

7 Department of Neurosurgery, Oslo University Hospital, Rikshospitalet, 0372 Oslo, Norway

8 Department of Neurosurgery, National Hospital, Rigshospitalet, 2100 Copenhagen, Denmark

Correspondence to: Olgerta Asko

E-mail: olgerta.asko@psykologi.uio.no

Highlights:

- Orbitofrontal lesions reduce auditory MMN (i.e., prediction error) to unpredicted stimuli at the local level.
- Orbitofrontal lesions reduce local and global level auditory deviance (i.e., prediction error) response, as manifested by diminished and delayed MMN and P3a.

Keywords: frontal lobe lesion; deviance detection; prediction error; prediction hierarchy; auditory perception; EEG

Abstract

Orbitofrontal cortex (OFC) is classically linked to inhibitory control, emotion regulation and reward processing. Recent perspectives propose that the OFC also generates predictions about perceptual events, actions, and their outcomes. We tested the causal involvement of the OFC in detecting violations of prediction at two levels of abstraction (i.e., hierarchical predictive processing) by studying the event-related potentials (ERPs) of patients with focal OFC lesions (n = 12) and healthy controls (n = 14) while they detected deviant sequences of tones in a Local-Global paradigm. The structural regularities of the tones were controlled at two hierarchical levels by rules defined at a local (i.e., *between tones within sequences)* and at a global (i.e., *between sequences*) level. In OFC patients, ERPs elicited by standard tones were unaffected at both local and global levels compared to controls. However, patients showed an attenuated mismatch negativity (MMN) to local prediction violation, as well as a diminished and delayed MMN/P3a complex to the combined local and global level prediction violation. Importantly, the subsequent P3b component to conditions involving violations of prediction at the level of global rules was preserved in the OFC group. The altered magnitudes and time courses of MMN/P3a responses after lesions to the OFC indicate fundamental impairments in detecting violation of auditory regularity at two hierarchical levels of stimuli abstraction.

Introduction

The orbitofrontal cortex (OFC) is linked to multiple high-level cognitive processes including inhibitory control,[1-3] goal-directed attention,[4-6] recent[7-9] and temporal context[10] memory and working memory (WM) maintenance,[11-15] all supporting pivotal involvement of the OFC in decision-making.[16-20] Extensive research has highlighted a key role of the OFC in outcome monitoring and evaluation (e.g.,[6,20,21]), and the signaling of reward value.[22-26] Patients with OFC damage typically demonstrate difficulty in learning from previous errors, often combined with reduced sensitivity to future consequences.[16,27-29] However, studies using tasks where outcomes do not have a clear emotional or motivational value support the idea that the OFC

forms representations of the environment that extend beyond reward.[25,30-32] A recent proposal is that OFC generates specific predictions about impending events, such as their identity and features, and uses relevant contextual and temporal attributes to allow continuous updating of rules.[33-35] This emerging view of OFC in monitoring the environment requires predicting events and outcomes but also noticing violations of expectation, that is, prediction errors (PEs).[36] Notably, animal[37-39] and human[40-42] studies have reported a role of the OFC in signaling PEs, but its involvement in the generation of PEs at different levels of content and temporal complexity remains largely unknown.

Noticing violations of expectation may occur across all levels of extended brain systems and be implemented in a hierarchical manner, such that higher-level structures predict inputs from lower-level ones through top-down connections, and error signals are sent back through bottom-up connections to update the current model of the environment.[43-46] According to the predictive coding hypothesis, the brain continually formulates predictions, or hypotheses, about sensory inputs and tests them against incoming sensory signals. The bottom-up information is not the input itself, but the interaction between the prediction and the actual sensory input (i.e., PE).[44,47-50] This framework might be extended to account for the organization of brain regions underlying higher cognitive processes, such as the frontal lobes. Indeed, predictive coding computational models have implicated the prefrontal cortex (PFC) in higher-order predictions and PE processing.[51-55] Studies addressing the role of subregions of PFC in predictive processing are sparse. The dorsal part of medial PFC (dmPFC) is reported to be specialized for reporting error as a deviation from predicted events.[56] The ventral part of medial PFC (vmPFC), i.e., OFC, has been proposed to integrate perceptual input from cortical and subcortical areas, together with memories of previous stimuli, to determine the current task context.[35] DmPFC and OFC subregions likely interact,[57] but the nature of the interplay and the specific role of the OFC remains to be delineated.

Numerous electrophysiological studies have used the predictive coding framework to explain the event-related potentials (ERPs), including the mismatch negativity (MMN) and P3 complex, as PE signals.[51,53,58-63] The fronto-centrally distributed, early (100-250 ms) MMN is usually elicited by an infrequent tone that differs in its acoustic properties (e.g., pitch, loudness) from a monotonous sequence of preceding frequent tones and persists in the absence of attention.[64,65] Within the predictive coding framework, the MMN is interpreted as an early PE signal arising from prediction violation due to a top-down predictive contribution.[47,53,60,66,67] In agreement with a hierarchical model transmitting predictions in a top-down fashion to lower

sensory areas are the findings of fMRI, scalp- and intracranial EEG studies showing MMN generators in the superior temporal planes bilaterally (i.e., primary auditory cortices and superior temporal gyri), in bilateral prefrontal cortices (i.e., inferior frontal gyri), as well as the inferior circular sulcus of the insula.[53-55,68-77] The distinct contribution of each part of this network, especially the prefrontal component, is not clear.

A positive polarity P3 complex (P3a and P3b), sensitive to the detection of unpredictable auditory events, is elicited after the MMN (e.g.,[58,59,62,78-80]). The earlier and more fronto-centrally distributed P3a is evoked by infrequent rare or novel stimuli,[81] and is weakly affected by voluntary attention.[82] It is typically interpreted as reflecting an involuntary attentional reorienting process,[83] related to the ventral attention network.[84-86] The P3b, with a centro-posterior maximum, is associated with context updating in WM,[81,87,88] allocation of attentional resources to stimulus evaluation,[89] and is dependent on limited-capacity attention and conscious awareness.[78,90,91] Lesion studies indicate that PFC integrity is necessary for the generation of the P3a,[92-95] whereas the hippocampus, parietal and frontal cortices are associated with P3b generation.[89,96-98]

Early studies using simple oddball tasks showed diminished MMN elicited by deviant tones within sequences of standard tones.[99,100] In the same vein, PFC injury reduced the amplitude of the frontally distributed P3a to unexpected novel auditory stimuli, whereas the parietally distributed P3b to detected deviants remained intact.[92,93,101] Løvstad et al.[101] reported attenuation of the P3a to unexpected novel environmental sounds after damage to either lateral PFC (lPFC) or OFC. Moreover, Solbakk et al.[102] showed that the N2b-P3a complex elicited by unexpected auditory sensory outcomes of self-initiated actions in OFC patients did not differ as clearly from the response to expected outcomes as for the healthy controls. Altogether, these findings indicate that OFC integrity might be necessary for the generation of the auditory MMN and P3a and support the idea that the OFC is involved in predicting different types of perceptual events and outcomes, monitoring ensuing sensory inputs, as well as noticing and evaluating violations of expectation.

Given the suggested involvement of OFC in predicting perceptual events and noticing violations of expectation (i.e., PEs), this study investigates whether the OFC is causally involved in the detection of PEs while processing auditory stimuli at two levels of abstraction. To this aim, we manipulated both the local and global auditory features of the environment by using a novel variant of the oddball paradigm originally devised by Bekinschtein et al.[78]. The

paradigm allows probing of hierarchical predictive processing by simultaneously violating expectations at two processing levels and time scales: A low "local" level with a short timescale (i.e., tone-onset asynchrony: 150 ms) and a higher "global" level with a longer timescale (i.e., sequence-onset asynchrony: seconds). At the local level, the regularity is determined by the transition probability (i.e., the probability with which a given stimulus follows another) *between tones within sequences*, while at the global level, the regularity is established by the transition probability *between sequences* as they unfold over a longer time-frame. The factorial (2x2) structure of the paradigm enables measuring predictive processing at one level along with the feed forwarding of PEs to the next level, as well as the interaction between processing levels (i.e., PEs at both local and global level). By dissociating neural responses elicited at hierarchically nested levels of acoustic regularity at two timescales, the paradigm has provided evidence for hierarchical stages in auditory processing linked to the MMN and P3 complex in the healthy human brain.[51,58,62,80] We first extended knowledge about the electrophysiological modulations (i.e., ERPs) elicited by auditory deviance processing at the "local" and "global" level by studying the interaction of these processing levels with the new "local+global" level condition in a cohort of healthy adults. We then examined the impact of OFC injury on these ERP markers by comparing healthy adults to patients with OFC lesions. Based on previous findings in oddball tasks manipulating local levels only, we expected attenuated MMN amplitude following OFC lesions. Because the OFC has been implicated in generating predictions about perceptual events and actions, we predicted dampened amplitudes of the P3 complex, which has been linked with deviance processing at a higher (i.e., "global") hierarchical level.

Materials and methods

Participants

Twelve (12) patients with lesions in the OFC and fourteen (14) healthy control participants (CTR) were enrolled in the experiment. CTRs were recruited by advertisement and personal contact, whereas patients were recruited through the Department of Neurosurgery at Oslo University Hospital. Inclusion of patients was based on the presence of focal frontal lobe lesions as indicated on pre-existing structural computer tomography (CT) and/or magnetic

resonance imaging (MRI) scans. Among the OFC group, ten had bilateral damage, and two had unilateral damage. All patients were in the chronic phase of recovery, that is, at least 2 years' post-tumor resection or trauma. Details of the brain lesions are provided in Table 1. The study groups did not differ significantly regarding sex, age, years of education, or estimated IQ. IQ was estimated based on the Verbal Comprehension and Matrices subtests of the Wechsler Abbreviated Scale of Intelligence (WASI)[103] (Table 2).

Table 1. Characteristics of lesions to the OFC

	Etiology	Lesion size (cm^3)			BA (Left hemisphere)	BA (Right hemisphere)
OFC		Total	L	R		
1	Olfactory Meningioma	43.0	23.2	19.8	10, 11	10, 11
2	Traumatic Brain Injury	24.9	6.4	18.5	11	10, 11, 47
3	Traumatic Brain Injury	157.4	59.8	97.6	8-11, 32, 45-48	6, 8-11, 24, 32, 44-48
4	Olfactory Meningioma	117.9	56.4	61.5	9-11, 32, 46, 47	10, 11, 32, 45-47
5	Olfactory Meningioma	6.6	3.2	3.4	11	11
6	Olfactory Meningioma	8.6	3.1	5.4	11	10, 11
7	Olfactory Meningioma	8.8	1.3	7.5	11	11, 47
8	Olfactory Meningioma	3.7	3.7	0	10, 11	_
9	Olfactory Meningioma	85.7	55.1	30.6	9-11, 25, 32, 46, 47	10, 11, 47
10	Olfactory Meningioma	109.0	48.8	60.3	10, 11, 32, 46, 47	9-11, 32, 45-47
11	Low Grade Glioma	6.4	0	6.4	_	10, 11
12	Olfactory Meningioma	32.6	10.1	22.5	11	10, 11, 25

Etiology, size (L, left; and R, right hemisphere), and affected Brodmann Areas (BA) for each hemisphere. The sign "_" is used when no lesion was present in a given hemisphere. Lesions that comprise < 0.2 cm^3 in any given BA are not reported.

Table 2. Demographics per group

Demographics	CTR	SD	OFC	SD	Stat.
N	14		12		
Gender (females: males)	8:6		8:4		
Age years, mean (range)	47.6 (34-66)	10.3	47.9 (27-61)	11.7	ns
Education years, mean (range)	16.1 (13-21)	2.0	15 (9-21)	3.1	ns
Total IQ, mean	115.4	10.3	112.2	8.5	ns

Comparison of the age, years of education, and IQ between the two groups (One-Way ANOVA). Values given are means, with standard deviation (SD). The mean value for total IQ is given in IQ scores. CTR, healthy control group. OFC, group with lesion to the orbitofrontal cortex. ns, the statistical test was not significant.

All participants gave written informed consent before participating in the study. Healthy controls received 400 NOK (approximately 50 USD) for participation in the entire research project (neuropsychological assessment, EEG recording, and MRI scanning). Patients participated in conjunction with clinical follow-ups at the hospital's outpatient clinic. Their travel and accommodation expenses were covered. The study design and protocol were approved by the Regional Committees for Medical and Health Research Ethics, South-East Norway as part of a larger study. The study was conducted in accordance with the principles stated in the Declaration of Helsinki.

Lesion mapping

Lesion mappings were based on structural MRI scans obtained after study inclusion and verified by the neurologist and the neurosurgeon in the research group (R. T. K, and T. R. M). Lesions were manually outlined on Fluid Attenuated Inversion Recovery (FLAIR) sequence images (1 × 1 × 1 mm^3 resolution) for each participant's brain using MRIcron2 (www.mccauslandcenter.sc.edu/mricro /mricron/). High-resolution T1-weighted images were used to help determine the borders of the lesions when required. Each participant's brain was extracted from the T1 image using the FSL Bet algorithm (FSL3) and then normalized to the Montreal Neurological Institute MNI-152 template space using the Statistical Parametric Mapping software (SPM12: www.fil.ion.ucl.ac.uk/spm/) unified segmentation and normalization procedures, while including the drawn lesions as masks. In addition, the transformation matrix was applied to the individual participant's FLAIR and lesion mask images. Figure 1 depicts the aggregate lesion reconstructions for the OFC group and the average percentage of damaged tissue within each Brodmann area (BA) per hemisphere.

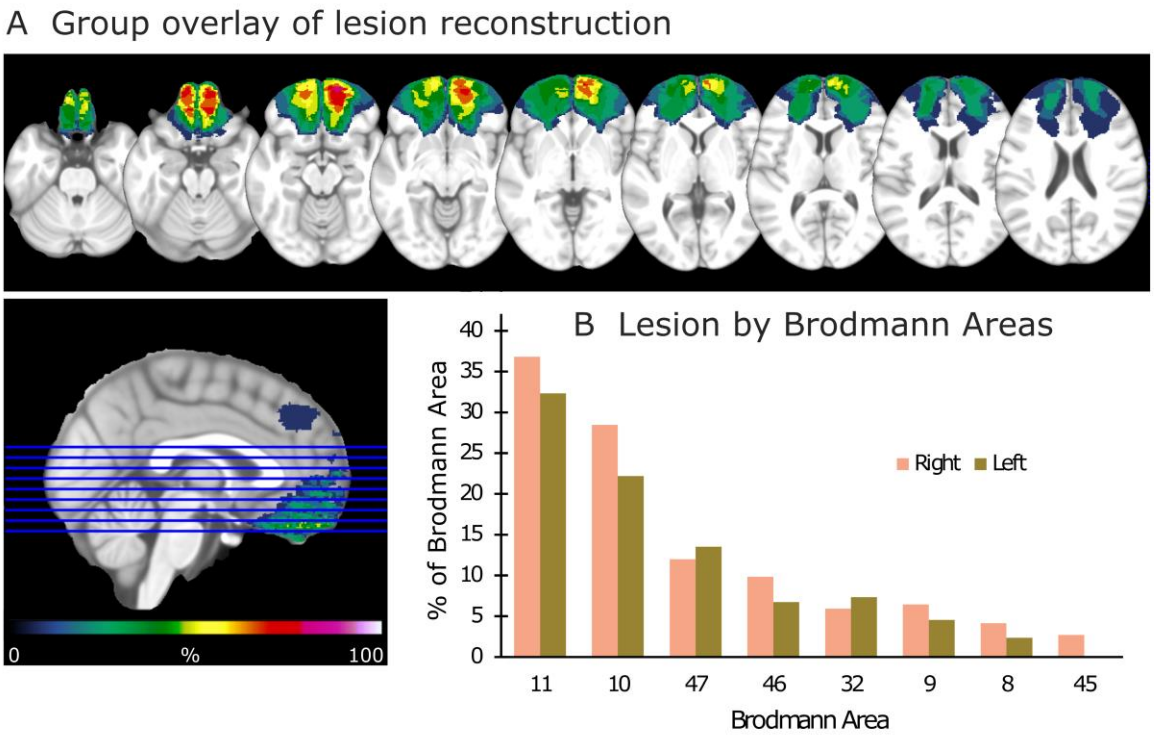

Figure 1. Lesion reconstruction for the group with OFC damage. (A) Aggregate lesion overlay maps in axial view. The color code (from 0 to 100%) for the group overlay indicates the percentage of shared lesion coverage across patients. The redder the color, the greater the lesion overlap. Neurological convention is used with the right side of the brain being on the right side of the image and vice versa. **(B)** Average percentage of damaged tissue within each Brodmann Area (BA) per hemisphere. BAs with less than 2% damage are not presented.

The Local-Global paradigm and procedures

Two tones composed of three sinusoidal tones (tone A: 440, 880, and 1760 Hz; tone B: 622, 1244, and 2488 Hz) were synthesized. Each tone was 50 ms long, with 7 ms rise and fall times. Sequences of four or five such tones were delivered with a fixed stimulus onset asynchrony (SOA) of 150 ms. Each sequence's SOA was randomly drawn from a uniform distribution between 1350 and 1650 ms (Figure 2A). Three different types of sequences were presented: (i) sequences comprised by five identical tones AAAAA or BBBBB (jointly denoted by **xx**), (ii) sequences comprised by four identical tones and a fifth different tone AAAAB or BBBBA (jointly denoted by **xy**), or (iii) sequences comprised by four identical tones AAAA_ or BBBB_ (jointly denoted by **xo**).

Three block types were defined: Regular (xX), Irregular (xY), and Omission (xO). In the present set of analyses, the Block xO were not further examined. Similar to Bekinschtein et al.,[78] each block of trials started with the repetition of 20 identical sequences of tones to establish the block's global rule. These were followed by 120 trials in each block. **Block xX**: 75% **xx** sequences referred to as **xx | xX** trials and 12,5% **xy** sequences referred to as **xy | xY** trials. **Block xY**: 75% **xy** sequences referred to as **xy | xY** trials and 12,5% **xx** sequences referred to as **xx | xY** trials. 12,5% of **xo** sequences were included in Block xX and Xy (see Figure 2B).

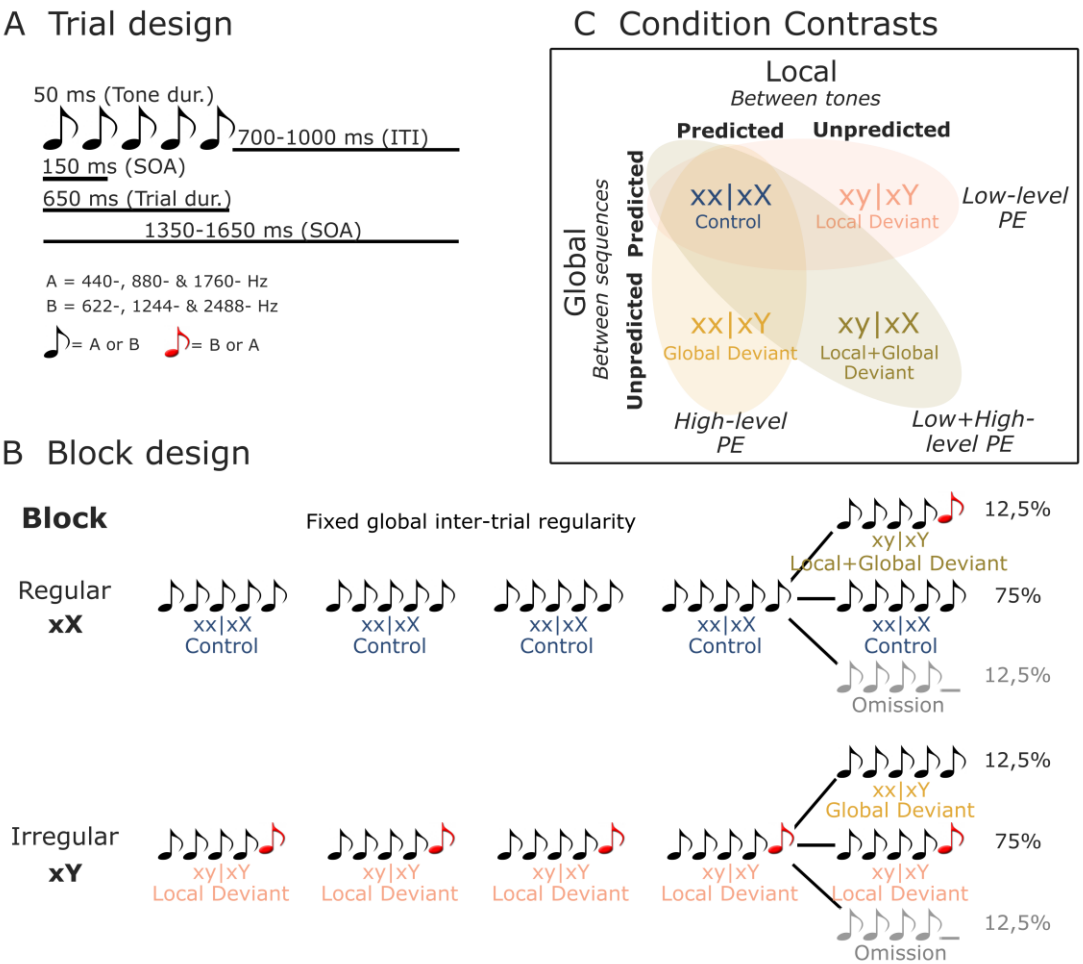

Figure 2. Illustration of stimuli and experimental design. (A) On each trial, five or four complex tones of 50 ms-duration each were presented with a fixed SOA of 150 ms. Two types of tones were used to generate these trials: tone A (composed of 440-, 880-, and 1760-Hz sinusoidal tones), and tone B (composed of 622-, 1244-, and 2488-Hz sinusoidal tones). **(B)** Each block started with 20 frequent sequences of tones to establish the block's global rule. In

regular xX blocks, standard sequences (75%) consisted of five repetitions of the same tone (i.e., xx | xX or Control trials). These were interspersed with rare local deviant sequences (12.5% each) where the fifth sound was either different in frequency type (i.e., xy | xX or Local+Global Deviant trials), or was omitted. The irregular xY blocks were similar, except that the standard sequences (75%) had a fifth sound differing in frequency type (i.e., xy | xY or Local Deviant trials), interspersed with rare (12.5%) local standard sequences (i.e., xx | xY or Global Deviant trials), or omission sequences. **(C)** By contrasting Control (xx | xX) trials with Local Deviant (xy | xY), Global Deviant (xx | xY) and Local+Global Deviant (xy | xX) trials, we isolate low-level, high-level and combined low- and high-level Prediction Error (PE) responses, respectively. dur., duration; ITI, Inter-Trial Interval; SOA, Stimulus Onset Asynchrony.

The experiment included two experimental sessions with 12 blocks in total (6 blocks of trials in each session, and each block type was presented twice where tones A and B were swapped, making a total of 1440 trials). The experimental blocks (of ~3-min duration each) were randomized across sessions and participants, except that the first block of each session was always Block xX. The paradigm enables the statistical contrast of trials that have the same physical stimulus properties, but differ in their stimulus transition probabilities and therefore in their predictability. The task does not entail any symbolic reward and no performance feedback is provided. Sound presentation was controlled with MATLAB (R2018a, MathWorks Inc., Natick, MA, USA), using the Psychophysics Toolbox version 3 (Kleiner, Brainard, & Delli, 2007).

Participants were seated comfortably in a Faraday-shielded room in front of a LCD monitor with a 60-Hz refresh rate placed at a distance of ~70 cm from the participant while presented with auditory stimuli. Stimuli were delivered through speakers on the side of the screen at a comfortable volume. Participants were instructed to attend to the auditory stimuli and count any rare/uncommon sequences. At the end of each block, participants reported this count in a data sheet before continuing the experiment. Hence, we expected participants to attend to and extract the global rule that characterized deviant sequences.

EEG acquisition and pre-processing

EEG was recorded at a 1024 Hz sampling rate using a 64-channel Active Two system (BioSemi, Amsterdam, Netherlands) with active electrodes placed in accordance with the International 10-20 system.[104] In addition, six external electrodes were used, including two electrodes placed above and below the right eye and two placed at the right and left outer canthus (vertical and horizontal EOG channels, respectively). The last two electrodes were placed on the right and left earlobes for offline re-referencing.

We used the FieldTrip toolbox[105] for MATLAB (R2018a, MathWorks Inc., Natick, MA, USA) for offline EEG data processing. EEG data were re-referenced to averaged earlobes, and the linear trend was subtracted. The continuous EEG data were then high-pass filtered back and forward (zero-phase) with an infinite impulse-response (IIR) Butterworth filter (order: 3), half-amplitude cutoff at 0.01 Hz. Spectral interference by power line noise was ameliorated by using the method of spectrum interpolation,[106] targeting the line noise frequency (50 Hz) and its first four harmonics. The continuous data were visually inspected and noise-contaminated channels and segments were identified (e.g., large muscle artifacts). The sample information of the noisy segments was saved for later rejection of epochs overlapping with these segments. Bad channels were removed before running an independent component analysis (ICA). The ICA was used to identify and then manually remove blinks and horizontal eye movements (ocular components) in the non-epoched data. Rejected channels were subsequently interpolated from the neighboring electrodes using spherical spline interpolation.[107]

Data analysis

Behavioral analysis

Behavioral data were collected in the form of a written report of the number of rare/uncommon sequences of tones detected (i.e., global deviants) per block. For each participant, we computed and reported the average percentage of errors over blocks, which is the deviation (positive or negative) relative to the actual number of presented global deviants.

Statistical analysis of event-related potentials

The pre-processed data were segmented into epochs of -2400 ms to 1800 ms relative to the onset of the last tone presentation and used for further analyses. Epochs in the habituation phase

(i.e., first 20 trials) of all blocks were excluded from further analysis. ERPs were calculated by averaging the stimulus-locked epochs for each condition. Prior to averaging, epochs were down-sampled to 512 Hz and baseline corrected relative to the mean activity -600 to -150 ms before the onset of the last tone.

To investigate deviance processing, we hypothesized an internal model with two hierarchical levels forming predictions and generating PEs that interact within and across levels - based on the hierarchical predictive coding model of local and global novelty proposed by Chao et al.[108]. The internal model generates predictions based on the statistical properties of the auditory stimuli. In accordance with the predictive coding theory, on Control (xx | xX) trials, the fifth tone "x" is predicted by a low-level prediction, and thus no PE should be elicited. In contrast, on Local Deviant (xy | xY) trials, enhanced low-level PEs arise, because the last tone "y" violates the transition probability established by the prior sequence of xxxx. High-level predictions anticipate these local violations, and thus high-level PEs are not expected to be elicited. On Global Deviant (xx | xY) trials, presumably only high-level PEs occur, caused by the unpredicted absence of tone "y", or more precisely, the absence of low-level PEs is unpredicted by the high level. Finally, on Local+Global Deviant (xy | xX) trials, PEs arise at a low level of processing since the expected tone "x" is replaced by the tone "y". In addition, these PEs, not anticipated by the global rule, activate a higher hierarchical level and elicit high-level PEs.

EEG-derived ERPs for the four conditions of interest (i.e., Control, Local Deviant, Global Deviant and Local+Global Deviant) were separately averaged to assess the neuronal markers of deviance processing. Furthermore, we evaluated three main condition contrasts. By contrasting Control (xx | xX) and Local Deviant (xy | xY) trials, we isolate the **Local Deviance** or low-level PE response, which arises when only local regularities are violated (i.e., a local deviance response predicted by the global rule). Contrasting Control and Global Deviant (xx | xY) trials isolates the **Global Deviance** or high-level PE response unaffected by local deviancy (i.e., a response to a stimulus that is unpredicted by the global rule but predicted at the local level). Finally, by contrasting Control and Local+Global Deviant (xy | xX) trials, we examine the **Local+Global Deviance** response or the combined effect of low- and high-level PE that occurs when both local and global regularities are violated (i.e., a local deviance response that is unpredicted by the global rule) (Figure 2C).

Pairs of experimental conditions were compared using a non-parametric cluster-based permutation method implemented in the FieldTrip toolbox addressing the multiple comparisons issue.[109] Cluster statistics were obtained by summing the t-values that were adjacent in space and time above and below a threshold level (two-sided t-test with alpha level 0.05). The cluster p-value was then obtained by comparing the cluster statistic to a null distribution statistic obtained by randomly switching condition labels within average participant responses 1000 times. The clusters were considered as significant when the sum of t-values exceeded 97.5% or were below 2.5% of the null distribution. Cluster-based permutation dependent samples *t*-tests were computed between 0 and 800 ms after the onset of the fifth tone for all the main condition comparisons. Tests were computed for the CTR and the OFC group separately. In a second step, to check for differences in the ERPs between the two groups, we ran the same cluster-based permutation approach contrasting each of the four conditions of interest between the two groups using independent samples *t*-tests. The cluster-based permutation independent samples *t*-tests were computed in the latency range of each component, which was based on the statistical analysis of the CTR and OFC group condition contrasts.

For component latency estimation, we used the 50%-area latency method,[110,111] which calculates the time point where an ERP component has reached the 50% of its area under the curve. Area latency reflects the median latency of a component, which is considered a more reliable measure than the traditional peak latency.[110,111] Component area was defined as the region bounded by the entire time window of the ERP component. To avoid missing component activity in individuals, we selected a broad time window (i.e., Local Deviance MMN: 50-150 ms and P3a: 140-350 ms; Local+Global Deviance MMN: 50-220 ms for the CTR and 50-250 ms for the OFC group, P3a: 180-450 ms for the CTR and 180-500 ms for the OFC group, P3b: 380-800 ms; Global Deviance P3b: 380-800 ms). For statistical tests on differences between the two groups in component latencies, independent samples t-tests were performed for each component of interest and each condition in the five midline electrodes (i.e., Fz, FCz, Cz, CPz, Pz).

Results

Behavioral performance

Participants from both groups performed the task properly with an average error rate of 10.45% (SD 9.27) for the healthy control participants (CTR) and 13.99% (SD 8.35) for the OFC lesion patients (OFC). There was no statistically significant difference between the counting performance of the two groups [$t(24) = -1.014$, $P = 0.814$].

EEG results

Local Deviance response – MMN and P3a components

Analysis of the Local Deviance response revealed that ERPs to local-level unpredicted tones (xy│xY trials) differed significantly from local-level predicted tones (xx│xX trials), where both sequences are predictable at the global level. Both groups showed condition differences corresponding to a negative cluster in the data at 67-128 ms (i.e., MMN) for the CTR group [$t(13) = -6633.65$, $P = 0.012$, 61/64 channels], and at 73-131 ms for the OFC group [$t(11) = -3734.49$, $P = 0.035$, 41/64 channels]. This was followed by a positive cluster at 143-313 ms (i.e., P3a) for the CTR group [$t(13) = 24808.43$, $P < 0.001$, 60/64 channels], which extended from 145 to 344 ms for the OFC group [$t(11) = 21796.75$, $P < 0.001$, 58/64 channels].

Testing for group differences was done in the time range of the MMN (i.e., from 50 to 150 ms), based on the statistical analysis of the CTR and OFC group condition contrasts. Analysis of the response to local-level unpredicted tones (xy│xY trials) revealed a reduced MMN for the OFC patients compared to the CTR in a time window from 73 to 110 ms [positive cluster: $t(25) = 1396.79$, $P = 0.028$, 39/64 channels]. We also checked for group differences in the condition difference waveforms (i.e., xy│xY - xx│xX trials), which yielded similar results [$t(25) = -1090.62$, $P = 0.02$]. However, the groups did not differ significantly in the time range (i.e., 140 to 350 ms, based on the statistical analysis of the CTR and OFC group condition contrasts) of the P3a (positive cluster: $P = 0.22$, negative cluster: $P = 0.53$). Latency analysis for the MMN and P3a components did not show statistically significant differences between the two groups. Interestingly, responses to the standard tones predicted at both levels (xx│xX trials) did not diverge significantly between the groups (positive cluster: $P = 0.79$, negative cluster: $P = 0.51$). See Figure 3 for a visual representation of the ERP waveforms of the CTR and OFC groups.

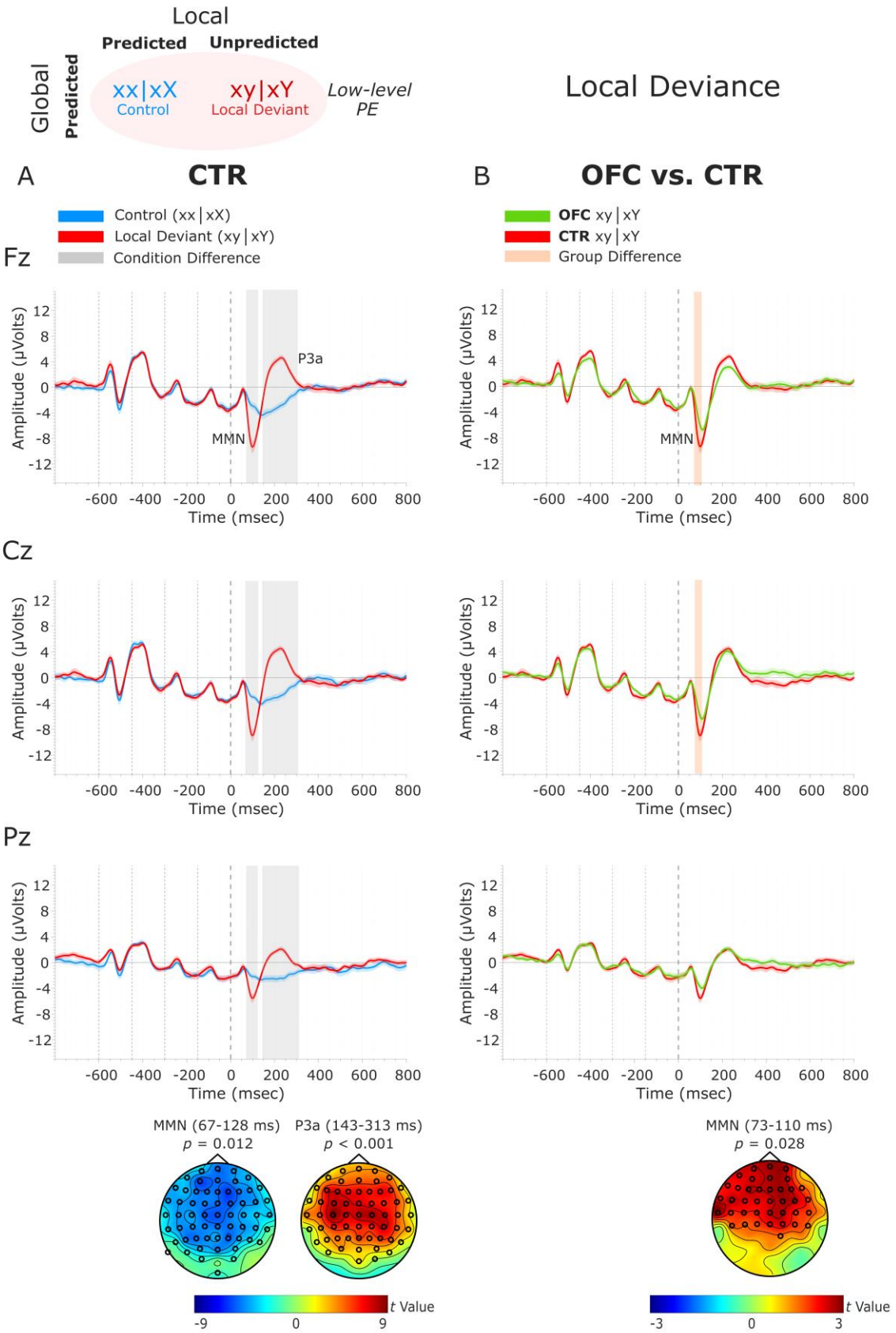

Figure 3. Local Deviance ERPs. (A) Local Deviance Response CTR. To the left, healthy control participants' grand average ERP waveforms at midline electrodes (from top to bottom:

Fz, Cz, Pz). ERPs from the processing of (standard) tones predicted at both levels (Control: xx | xX trials) are in blue, and ERPs from the processing of (deviant) tones unpredicted at the local level (Local Deviant: xy | xY trials) are in red. Gray shaded bars indicate times when the electrode was part of a cluster showing significant within-group condition differences. At the bottom, the topographic scalp maps represent the statistical difference values for the t-contrast of the two experimental conditions computed for the time window corresponding to the cluster with significant differences. **(B) Group Differences (CTR vs. OFC).** To the right, CTR and OFC grand average ERP waveforms at the same midline electrodes. ERPs from the processing of tones unpredicted at the local level (Local Deviant: xy | xY trials) are in red for CTR and in green for OFC. Orange shaded bars indicate times when the electrode was part of a cluster showing significant differences between the groups. At the bottom, the topographic scalp map represents the statistical difference values for the t-contrast of the two groups computed for the time window corresponding to the cluster showing differences. MMN and P3a latencies did not show statistically significant differences between groups. Dashed lines at -600, -450, -300, -150, and 0 ms depict tone onsets. Shaded areas around the waveforms represent the standard error of the mean (SEM).

Global Deviance response – P3b component

We examined the presence of only a high-level deviance response, i.e., Global Deviance, by comparing globally unpredicted tones (Global Deviant: xx | xY trials) with globally predicted ones (Control: xx | xX trials), while keeping the local level predictions fulfilled (i.e., tones were locally predicted). Results revealed a significant condition effect captured by a positive cluster at posterior electrodes, which lasted from 381 to 714 ms for the CTR [$t(13) = 10521.05$, $P = 0.009$, 33/64 channels], and from 419 to 799 ms for the OFC group [$t(11) = 13120.99$, $P = 0.01$, 51/64 channels]. This Global Deviance ERP response is long-lasting with no well-defined peak and has the classical posterior maximum scalp topography and latency of the P3b (Figure 4).

No statistically significant differences between the two groups were found in the time-window (i.e., from 380 to 800 ms, based on CTR and OFC group condition contrasts) of the P3b (positive cluster: $P = 0.61$, no significant negative cluster was detected). Latency analysis for the P3b component did not show statistically significant differences between the two groups.

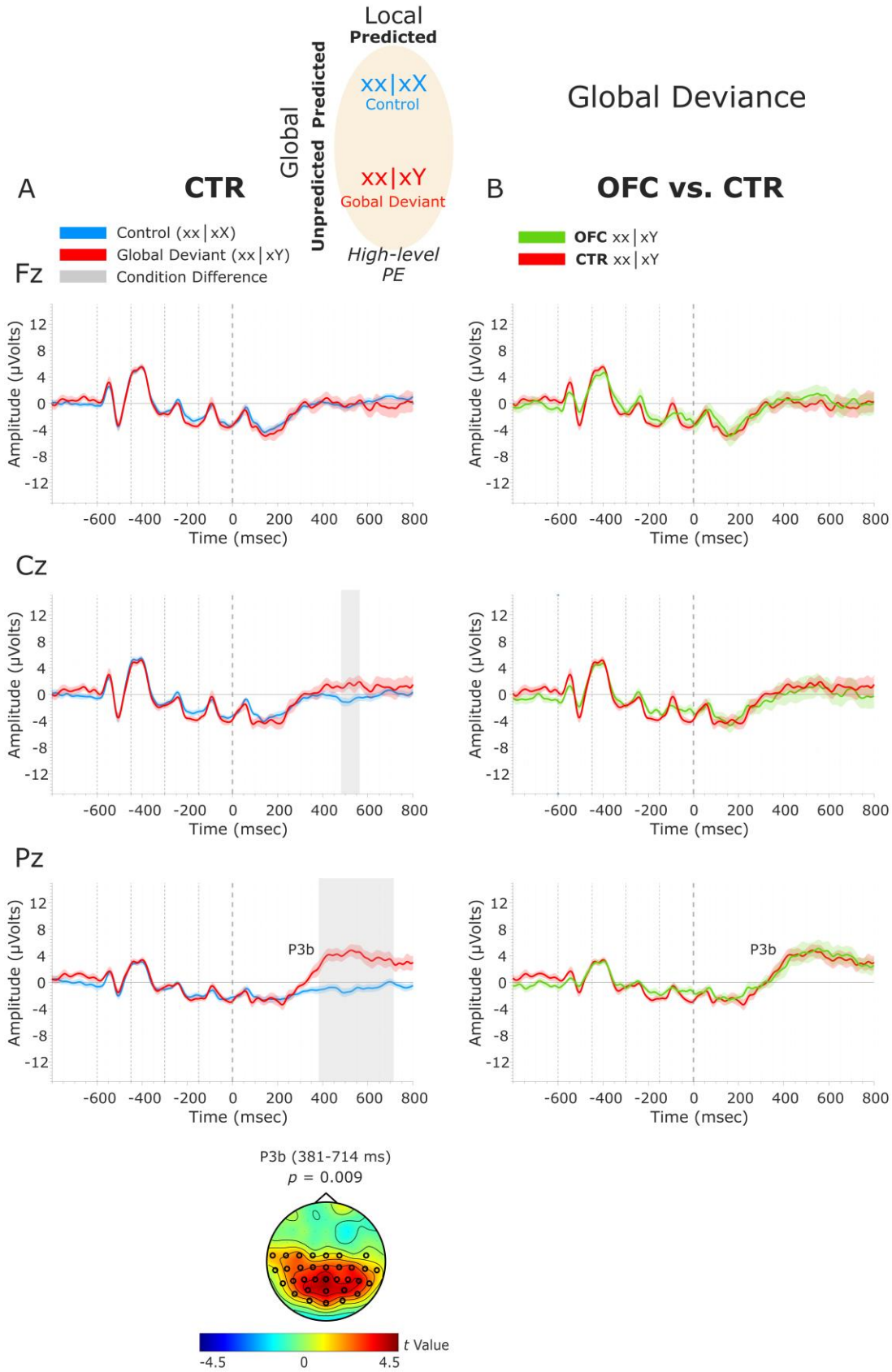

Figure 4. Global Deviance ERPs. (A) Global Deviance Response CTR. To the left, control participants' grand average ERP waveforms at three midline electrodes (from top to bottom:

Fz, Cz, and Pz). ERPs from the processing of (standard) tones predicted at both local and global levels (Control: xx | xX trials) are in blue, and ERPs from the processing of (standard) tones unpredicted only at the global level (Global Deviant: xx | xY trials) are in red. Gray shaded bars indicate times when the electrode was part of a cluster showing significant within-group condition differences. At the bottom, the topographic scalp map represents the statistical difference values for the T-contrast of the two experimental conditions computed for the time window corresponding to the cluster showing significant differences. **(B) Group Differences (CTR vs. OFC).** To the right, CTR and OFC grand average ERP waveforms at the same midline electrodes. ERPs from the processing of standard tones unpredicted at the global level (Global Deviant: xx | xY trials) are in red for CTR and green for OFC. P3b latency did not show statistically significant differences between groups. Dashed lines at -600, -450, -300, -150, and 0 ms depict tone onsets. Shaded areas around the waveforms represent the standard error of the mean (SEM).

Local+Global Deviance response – MMN, P3a, and P3b components

Finally, the analysis of the Local+Global Deviance responses resulting from the comparison of tones unpredicted (i.e., deviants) at both local and global level (Local+Global Deviant: xy | xX trials) with tones predicted at both levels (Control: xx | xX trials) revealed a main effect of condition for both groups. Here, a sequence of successive deviance-related ERPs, hereafter-termed "local+global" responses, was observed. Specifically, the CTR group showed a high-level deviance response (i.e., two-peak and long-lasting MMN) induced by a deviant tone (i.e., unpredicted by the local rule) that is also unpredicted by the global rule, as indexed by a negative cluster with a frontal scalp distribution at 71-186 ms [$t(13) = -7229.33$, $P = 0.016$, 59/64 channels]. Moreover, the OFC patients showed a similar MMN to unpredicted deviant tones at 67-139 ms, which did not reach significance when comparing with predicted standard tones [negative cluster: $t(11) = -3690.11$, $P = 0.068$]. Following the MMN, a P3 complex (composed of a frontally distributed P3a and a posteriorly distributed P3b response) was observed in CTRs, as indexed by a positive cluster extending from around 188 to 684 ms [$t(13) = 42019.65$, $P < 0.001$, 63/64 channels]. A similar P3 complex was found for the OFC patients as indexed by a positive cluster from 217 to 710 ms [$t(11) = 33590.81$, $P < 0.001$, 64/64 channels].

Group-level statistics performed on the MMN time-window (i.e., from 70 ms to 185 ms, based on CTR and OFC group condition contrasts) showed a trend-level reduced MMN for OFC patients compared to controls in a time-window between 81 and 106 ms [positive cluster: $t(25) = 588.31$, $P = 0.066$, 34/64 channels]. We also checked for group differences in the difference waveforms (i.e., xy | xX - xx | xX trials), which yielded similar results [$t(25) = -314.64$, $P = 0.068$]. The MMN was significantly delayed for the OFC group and it manifested 19.68 ms later in the central electrodes FCz [$t(24) = 2.26$, $P = 0.033$] and Cz [$t(24) = 1.78$, $P = 0.088$], but not the other electrodes (i.e., Fz, CPz and Pz).

We tested for group differences in the time window of P3a (i.e., from 180 to 485 ms after the onset of the fifth tone). Analysis of the response to Local+Global deviants revealed an attenuated P3a for OFC patients compared to CTRs in a time-window from 184 to 274 ms [negative cluster: $t(25) = -3730.34$, $P = 0.024$, 59/64 channels], and from 329 to 479 ms [positive cluster: $t(25) = 3063.91$, $P = 0.03$, 36/64 channels]. Latency analysis revealed that the P3a emerged 60.82 ms later, on average, in the OFC compared to the CTR group. This latency difference was significant for all the midline electrodes [Fz: $t(24) = 4.91$, $P < 0.001$; FCz: $t(24) = 4.64$, $P < 0.001$; Cz: $t(24) = 4.75$, $P < 0.001$; CPz: $t(24) = 3.46$, $P = 0.002$; Pz: $t(24) = 4.34$, $P < 0.001$]. Table 3 shows the 50% - area latencies for MMN and P3a components for the midline electrodes.

Table 3. 50%-Area Latency of the MMN and P3a for the Local+Global Deviant Response for the two groups

	MMN				P3a			
	Latency (SD)		Diff. (msec)	*P* value	Latency (SD)		Diff. (msec)	*P* value
	CTR	*OFC*			*CTR*	*OFC*		
Fz	127.40 (20.09)	138.28 (26.14)	10.88	0.242	279.88 (21.37)	334.90 (35.13)	55.01	< 0.001
FCz	127.54 (20.07)	148.21 (26.54)	20.67	0.033	280.02 (26.27)	332.78 (31.74)	52.76	<0.001
Cz	128.38 (19.57)	147.07 (33.21)	18.69	0.088	282.95 (28.77)	352.47 (45.17)	69.52	<0.001
CPz	129.07 (23.87)	139.67 (30.96)	10.89	0.330	283.79 (24.57)	347.59 (63.79)	63.80	0.002
Pz	130.61 (22.36)	149.19 (33.54)	18.58	0.105	292.58 (33.90)	355.57 (40.10)	62.99	<0.001

50%-area latency measures in milliseconds (msec) from the onset of the fifth tone for the MMN and the P3a components, separately for the healthy control participants (CTR) and the OFC lesion patients (OFC). Diff. is the latency difference between the two groups (OFC - CTR) given in msec; *P* values as a result of independent samples t-tests comparing the component's 50%-area latency between the two groups. Standard Deviation (SD) is given in brackets.

No statistically significant differences between the two groups were found in the time-window of the P3b (i.e., from 450 ms to 710, based on CTR and OFC group condition contrasts) for amplitude and latency analysis. Figure 5 illustrates these results.

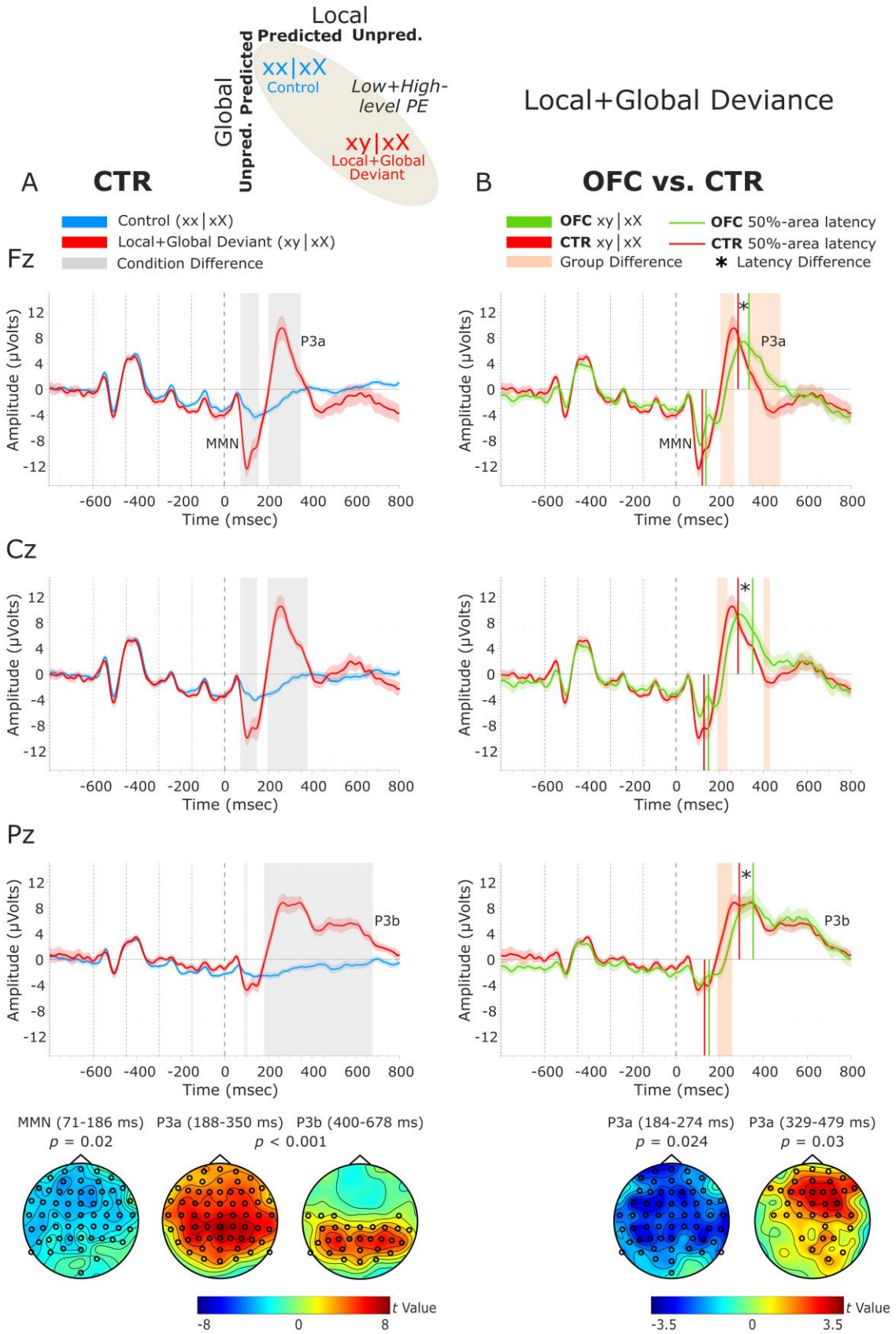

Figure 5. Local+Global Deviance ERPs. (A) Local+Global Deviance Response CTR. To the left, healthy control participants' grand average ERP waveforms at midline electrodes (from

top to bottom: Fz, Cz, Pz). ERPs from the processing of (standard) tones predicted at both local and global levels (Control: xx | xX trials) are in blue, and ERPs from the processing of (deviant) tones unpredicted at both levels (Local+Global Deviant: xy | xX trials) are in red. Gray shaded bars indicate times when the electrode was part of a cluster showing significant within-group condition differences. At the bottom, the topographic scalp maps reflect the statistical difference values for the t-contrast of the two experimental conditions computed for the time window corresponding to the cluster with significant differences. **(B) Group Differences (CTR vs. OFC).** To the right, CTR and OFC grand average ERP waveforms at the same midline electrodes. ERPs from the processing of (deviant) tones unpredicted at both local and global level (Local+Global Deviant: xy | xX trials) are in red for CTR and in green for OFC. Orange shaded bars indicate times when the electrode was part of a cluster showing significant differences between the groups. Vertical red lines indicate the 50%-area latency for the CTR group while vertical green lines indicate the latency for the OFC group for the corresponding components (i.e., MMN and P3a). Asterisks (*) denote latency significant differences. At the bottom, the topographic scalp maps represent the statistical difference values for the t-contrast of the two groups computed for the time window corresponding to the cluster with observed differences. Dashed lines at -600, -450, -300, -150, and 0 ms depict tone onsets. Shaded areas around the waveforms represent the standard error of the mean (SEM).

A complementary analysis comparing the processing of Local Deviant with Local+Global Deviant in the CTR group showed significant differences in both ERPs' amplitude (Supplementary Fig 1A) and latency (Supplementary Table 1). The OFC group analysis yielded similar results (Supplementary material). We also examined if the groups diverged in the difference waveforms Local+Global Deviant minus Local Deviant and found differences in both amplitude (Supplementary Fig 1B) and latency (Supplementary Table 2).

In summary, in both groups, local level deviant tones produced an early MMN followed by a frontally distributed P3a. Local level standard tones, which were unpredicted by the global rule, elicited only a posterior P3b. Local level deviant tones in sequences unpredicted by the global rule (i.e., local+global level deviants) produced a long-lasting MMN, followed by a P3 complex (frontal P3a and posterior P3b). In OFC patients, ERPs elicited by local level standard tones, both predicted and unpredicted by the global rule, were unaffected compared to CTRs. However, patients showed an attenuated MMN to local level deviant tones, as well as

attenuated and delayed MMN and P3a to local+global level deviant tones, while the P3b was unaffected.

Discussion

We examined the causal involvement of the OFC in detecting violations of predictions (i.e., PE) at the two hierarchical levels of the local-global paradigm. To achieve this, we studied the neurophysiological markers of auditory deviance processing in patients with focal OFC lesions and healthy controls while occasionally violating their predictions at a local (i.e., *between tones within sequence*) and at a global (i.e., *between sequences*) time scale. By attending to tone sequences and counting any rare sequences, we expected that participants would extract the global rule that characterized deviant sequences. The reported counts suggest that patients accomplished the counting properly despite their OFC damage. However, the ERPs findings showed that processing of auditory stimuli that violated predictions at the local level, even when these were predicted by the global rule, was affected by the OFC lesion. More notably the OFC lesion affected processing of stimuli that violated predictions at both the local and the global level. However, processing of predicted auditory stimuli at the local level, even when these were unpredicted by the global rule, was preserved in the OFC group. These results provide novel evidence about the role of the OFC in detecting violation of auditory prediction at two levels of stimuli abstraction/time scale.

OFC lesions affect the processing of local level deviants

At the local level (xy│xY), deviant tones generated a low-level PE response indexed by two successive ERP components within an early 70-310 ms window: First a MMN, which was followed by a P3a. These ERP responses for the healthy control participants were comparable to those reported in previous studies using a similar experimental design.[51,58,59,62,78] These studies have interpreted the short-term (i.e., local level) MMN as a bottom-up PE signal, which indexes the amount of information in each deviant event and is explained away by top-down prediction signals. The P3a, which is sensitive to the local status of the deviant tone, has also been reported in previous scalp-[51,59,78,80] and intracranial[79] EEG studies. It has been associated with the orienting of attention towards the unexpected local deviant tone, or the evaluation of its contextual novelty, i.e., how novel the tone is in global terms.[83] The OFC patients had ERPs

with similar morphology and scalp distribution as the controls, but the MMN amplitude was significantly attenuated at fronto-central sites. The MMN dampening adds to previous studies, which found reduced MMN to local-level auditory deviants after damage to the dlPFC.[99,100] The current findings show for the first time that the MMN elicited by local-level auditory deviants is also reduced in patients with lesions to the OFC, supporting the role of this area in detecting violations of expectations (e.g.,[36,40,41]).

OFC lesions affect the processing of local and global level deviants

Most studies using the local-global paradigm tested the global violation by pooling over all rare sequences of tones (i.e., xx | xY and xy | xX trials), which, as per our assumptions, contains two different types of PE signals. We split this classical global condition into Local+Global and Global Deviance (see Methods). The former requires detection of a deviant tone following a sequence of four identical tones (i.e., low-level PE) and concurrently identifying this rare sequence as a global deviant among frequent sequences (i.e., high-level PE). The latter requires detection of a rare sequence of five identical tones as a global deviant among frequent sequences (i.e., only high-level PE).

According to the predictive coding hypothesis, later stages in the predictive hierarchy, which integrate information over longer temporal windows, track more complex changes in sensory patterns.[58] Indeed, the detection of Local+Global" Deviance in this task evoked patterns of brain activity comprised of a "two-peak" and long-lasting MMN (70-185 ms) followed by a sustained positive polarity ERP, consisting of an early, frontaly-distributed P3a and a late, posteriorly-distributed P3b response. Previous research has shown that tone sequences with pitch deviations elicited both the MMN and P3 when participants were instructed to focus on the local rule (i.e., deviant tones). However, in contrast with our findings, the MMN was no longer elicited, while the P3 was maintained when participants were instructed to focus on the global rule (i.e., deviant sequences).[112] In the present study, participants were asked to focus on the global rule, but the MMN was still evoked after both local and local+global level pitch deviations. Interestingly, the MMN and P3a elicited by a combined local and global level violation were larger and longer-lasting than those elicited by a local level violation (see supplementary materials), which in predictive coding terms can be explained by a high-level prediction partially explaining away the low-level PE for the latter. Consistent with previous studies,[62,80] this finding indicates that violation of not only local, but also local+global regularity is reflected in the MMN. This is in contrast with studies suggesting that high-level

violations are indexed uniquely by P3 responses.[58,62,78,113,114] Overall, this is suggestive that low- and high-level PEs are dependent on- and interact with each other.

Moreover, the "two-peak" appearance of the MMN in the Local+Global Deviance condition, which is not present in response to the Local Deviance condition, may suggest overlapping of an "early MMN" with a succeeding N2b or "late MMN" component. Interestingly, the N2b has been linked with voluntary attention[64] and it is unaffected by changes in the temporal spacing of sounds. This is in contrast to the "early MMN", which has been associated with automatic and short-term processing of novelty.[115] In our study, an N2b along with a P3a may indicate a stronger influence of voluntary attentional resources engaged in the Local+Global Deviance processing (i.e., low- and high-level PE), where an accumulation of evidence on longer times scales is required. On the other hand, the first peak or "early MMN" would reflect accumulation of evidence based on short-lived echoic memory representation or, in predictive coding terms, an automatic, low-level PE response.

The OFC group generated the same pattern of ERP responses as the healthy controls, but the MMN and P3a to the Local+Global Deviance were attenuated and prolonged by approximately 20 ms and 60 ms, respectively, indicating that OFC lesion delays the processing of deviant tones, which belong in sequences unpredicted by the global rule. To our knowledge, only one previous study reported reduced P3a amplitudes in OFC patients performing an auditory novelty oddball task[101] and no studies have reported latency effects. In studies of lPFC lesion patients, frontal P3 reduction was explained as a deficit in the orienting response to unexpected and novel stimuli.[92,94,95] Here, we extend these findings by highlighting a role of the OFC in detecting deviant stimuli, which are unpredicted at the global level and therefore require integration of information over longer timescales and at a higher level of abstraction.

OFC lesions do not affect the processing of global level deviants (i.e., unexpected standards)

The detection of Global Deviance elicited exclusively a late posterior P3b for the control group. In line with this finding, a study using the same paradigm demonstrated that sequences of five identical tones, which were unpredicted by the global rule, evoked no MMN but a P3b-like response.[62] According to the authors, the fact that a sequence of five identical tones elicited a novelty signal when participants expected a different sequence suggested that the brain operates as a multilevel predictive system with P3b reflecting a high-level PE. Based on this assumption, we expected that OFC lesions would affect the P3b response as well. However,

our results showed that the posterior P3b was unaffected by OFC damage both in Local+Global and Global Deviance detection. One possible explanation is that P3b is elicited by target detection and not automatic deviance detection per se, i.e., specifically linked to the detection of events that are salient or important to the current goal and memory-related processes.[81,116,117] Note that as participants were instructed to count and memorize the total number of global deviations, these violations (i.e., xx | xY and xy | xX) were also the targets in the present study. Indeed, in oddball tasks, targets, but not other deviants, elicit large amplitude P3b responses associated with voluntary detection of infrequent and task-relevant stimuli.[96] Similar to our results, a MEG study showed that violations of global auditory regularities led to a later, more stable and long-lasting pattern of activity, which also engaged working memory in parietal and prefrontal areas.[118] Interestingly, when the same paradigm was used in patients suffering from disorders of consciousness, the P3 response to global novelty was only observed in patients who showed signs of consciousness.[78,119,120] The P3b response to Local+Global and Global Deviance could thus reflect downstream processes related to conscious access per se[121,122] and not a high-level deviant detection signal. Moreover, lesions in the lPFC[92,93,101] and the OFC[101] have been found to reduce the amplitude of P3a but not P3b, supporting normal target detection and suggesting that the OFC is not critical for P3b generation.

General Discussion

From the perspective of predictive coding, the MMN has been explained in terms of perceptual learning under hierarchical generative models of auditory input.[47,123] Over repeated presentations of standard stimuli, both intrinsic (within-area) and extrinsic (between-area) connections change in order to suppress PE by using top-down predictions. The MMN is interpreted as reflecting a cortical driven PE signal, which can be accounted for only by postulating a top-down predictive contribution.[47,53,60,66,67] Numerous studies have shown that the MMN has interacting generators in the superior temporal planes, as well as in the prefrontal cortex[68-73,124] and is best explained by deviant-induced suspension of neural adaptation within the primary auditory cortices, along with changes in temporo-frontal connections.[52-55,74] These findings support the idea of a hierarchy of internal models, which transmit predictions in a top-down fashion to lower sensory areas. Within this framework, the attenuated MMN in the OFC patients indicates, first, that the OFC may have a role in the neural circuitry underlying MMN generation and, second, that it may contribute to a top-down process that modulates the deviance detection system in the primary auditory cortices. The fact that the OFC patients do

not show reduced amplitudes while processing standard tones suggests that stimulus specific adaptation (SSA) is intact and that the processing of PE, which relies on top-down prediction signals, is more likely to be affected by the OFC lesion. Note that the OFC patients have a diminished MMN, but not an absolute absence of MMN. Overall, we suggest that the fact that the MMN elicited by the "local" and "local+global" violation was reduced in the OFC group may indicate impaired processes involved in connecting PEs at lower hierarchical areas with predictions at higher areas, thereby leading to a weakened PE signal.

Temporal information provided by scalp and intracranial ERP data converge in suggesting that P3a reflects a late stage of novelty processing, most likely related to the evaluation aspects of the involuntary orienting response.[125-127] P3a is also found to be elicited when the novel stimulus is potentially task-relevant[128] and strongly dependent on the context in which it is presented.[129] Interestingly, the P3a has been sourced localized to the same anterior cingulate and PFC network that is also involved in error processing.[130,131] This is indicative that responses to novelty actually reflect PEs, which may result in a brain response that generates the P3a.[132] In this study, the reduction and delay of P3a while processing deviant tones at the combined "local" and "global" level, indicates the contribution of OFC in a later stage of deviance processing. This later stage is thought to be based on top-down prior expectations and may consequently reflect high-level PEs. Thus, we suggest that the alteration of P3a in the OFC group could be due not only to an impaired orienting response, but also to a partial deterioration and/or a delay to detect and process violations of prediction (i.e., PE) at a higher level of abstraction. Indeed, the OFC has been linked with evaluation of novelty and information that violates expectations in order to regulate the individual's response to such new information.[36] For example, studies have implicated OFC in signaling predicted sensory features and external cues such as timing or probability.[24,34,133-136] This implies that OFC maintains a broad representation of available information (both sensory and unobservable information, such as abstract rules) that defines the situation or task at hand, potential actions, and their association to outcome expectations.

Experimental evidence, which has been reinterpreted in terms of predictive coding, suggests that the PFC contributes to a top-down process that modulates the auditory deviance detection system in the primary auditory cortices.[68,69] Specifically, the processing of deviants unpredicted by the global rule might aggregate information from distributed frontoparietal networks, subserving conscious access to the detected patterns and deviations therein.[137] However, the role of the OFC in this frontoparietal network is rarely studied. The altered ERP responses

observed in our OFC group are in line with previous observations of an intracranial EEG study in monkeys,[108] which reported high-level PE and prediction update signals primarily encoded in the frontopolar PFC (BA 10) and the dlPFC. The ventrolateral PFC (BAs 44, 45, 47) has also been found to be involved in the processing of high complexity auditory sequences[138] and sequence-order PEs.[139] Studies using the local-global paradigm showed high-level PEs confined to the vlPFC.[140,141] Interestingly, some of the same areas (i.e., BAs 10, 47, 45) were damaged in our OFC cohort. In a PET study, increased and selective modulation of activity within the OFC (i.e., BAs 11 and 13) was found to reflect the brain's response to stimuli that deviated from expectation.[142] Moreover, in a single neuron study, a population of neurons in BA 11 of the macaque monkey responded selectively to novel but not familiar stimuli and this response habituated very quickly and was long lasting.[143] As OFC's BA 11 is strongly connected with lateral prefrontal areas, it has been suggested that it is involved in capturing information that is novel relative to current experience and expectations, and linking this information to the higher cognitive processing occurring in the lPFC.[36]

On anatomic grounds, the OFC is unique among areas in the PFC with close connectivity to all five sensory modalities and bidirectional connections to areas relevant for memory and decision-making such as the hippocampus and the striatum.[144] This makes OFC suitable for supporting the formation of predictions that define the current task by using contextual and temporal structure in the environment to allow old rules to be disregarded so that new ones can be rapidly acquired.[34,35] Moreover, findings from lesion studies of time perception[102,145,146] proposed that an intact OFC plays a role in maintaining temporal information needed to sustain a stable map of task context for a longer time, which in turn is needed to optimize predictions.[33,134] Our findings support the idea that an intact OFC is necessary for holding an internal representation of the entire pool of sequences of auditory stimuli, sufficient to generate vigorous PE signals when violations of prediction are detected.

Conclusion

In this study, we tested the causal involvement of the OFC in detecting violations of prediction (i.e., PEs) at two hierarchical levels of task structural complexity. Our critical finding is that low-level PEs (i.e., processing of stimuli that are unpredicted at the local level) and combined low- and high-level PEs (i.e., processing of stimuli that are unpredicted at both the local and global level) were impacted by the OFC lesion. We conclude that the OFC may contribute to

a top-down predictive process that modulates the deviance detection system in the primary auditory cortices and may be involved in connecting PEs at lower hierarchical areas with predictions at higher areas. This study sheds new light on the poorly explored causal role of the OFC in hierarchical auditory predictive processing.

Acknowledgements

We are very thankful to all the patients and healthy controls who participated in this study. We acknowledge professor Per Kristian Hol, Intervention Center at Oslo University Hospital, for his valuable help with clinical evaluation of the MRI scans of patients and healthy controls.

Data availability

Data and all analysis algorithms will be provided on reasonable request by the corresponding author.

Competing interests

The authors report no competing interests.

References

1. Godefroy O, Cabaret M, Petit-Chenal V, Pruvo J-P, Rousseaux M. Control functions of the frontal lobes. Modularity of the central-supervisory system? *Cortex*. 1999;35(1):1-20.
2. Harlow JM. Recovery from the passage of an iron bar through the head. *History of Psychiatry*. 1993;4(14):274-281.
3. Picton TW, Stuss DT, Alexander MP, Shallice T, Binns MA, Gillingham S. Effects of focal frontal lesions on response inhibition. *Cerebral cortex*. 2007;17(4):826-838.
4. Badre D, Wagner AD. Selection, integration, and conflict monitoring: assessing the nature and generality of prefrontal cognitive control mechanisms. *Neuron*. 2004;41(3):473-487.
5. Luu P, Flaisch T, Tucker DM. Medial frontal cortex in action monitoring. *Journal of neuroscience*. 2000;20(1):464-469.
6. Walton ME, Devlin JT, Rushworth MF. Interactions between decision making and performance monitoring within prefrontal cortex. *Nature neuroscience*. 2004;7(11):1259-1265.
7. Barker GR, Bird F, Alexander V, Warburton EC. Recognition memory for objects, place, and temporal order: a disconnection analysis of the role of the medial prefrontal cortex and perirhinal cortex. *Journal of Neuroscience*. 2007;27(11):2948-2957.

8. DeVito LM, Eichenbaum H. Memory for the order of events in specific sequences: contributions of the hippocampus and medial prefrontal cortex. *Journal of Neuroscience*. 2011;31(9):3169-3175.
9. Shimamura AP, Janowsky JS, Squire LR. Memory for the temporal order of events in patients with frontal lobe lesions and amnesic patients. *Neuropsychologia*. 1990;28(8):803-813.
10. Duarte A, Henson RN, Knight RT, Emery T, Graham KS. Orbito-frontal cortex is necessary for temporal context memory. *Journal of Cognitive Neuroscience*. 2010;22(8):1819-1831.
11. Llorens A, Funderud I, Blenkmann AO, et al. Preservation of Interference Effects in Working Memory After Orbitofrontal Damage. *Frontiers in human neuroscience*. 2020;13:445.
12. Barbey AK, Koenigs M, Grafman J. Orbitofrontal contributions to human working memory. *Cerebral Cortex*. 2011;21(4):789-795.
13. Owen AM, McMillan KM, Laird AR, Bullmore E. N-back working memory paradigm: A meta-analysis of normative functional neuroimaging studies. *Human brain mapping*. 2005;25(1):46-59.
14. Wager TD, Smith EE. Neuroimaging studies of working memory. *Cognitive, Affective, & Behavioral Neuroscience*. 2003;3(4):255-274.
15. D'Esposito M, Postle BR, Rypma B. Prefrontal cortical contributions to working memory: evidence from event-related fMRI studies. *Executive control and the frontal lobe: Current issues*. 2000:3-11.
16. Bechara A, Damasio H, Damasio AR. Emotion, decision making and the orbitofrontal cortex. *Cerebral cortex*. 2000;10(3):295-307.
17. Bechara A, Damasio H, Tranel D, Anderson SW. Dissociation of working memory from decision making within the human prefrontal cortex. *Journal of neuroscience*. 1998;18(1):428-437.
18. Ernst M, Bolla K, Mouratidis M, et al. Decision-making in a risk-taking task: a PET study. *Neuropsychopharmacology*. 2002;26(5):682-691.
19. Hebscher M, Gilboa A. A boost of confidence: The role of the ventromedial prefrontal cortex in memory, decision-making, and schemas. *Neuropsychologia*. 2016;90:46-58.
20. Ullsperger M, von Cramon DY. Decision making, performance and outcome monitoring in frontal cortical areas. *Nature neuroscience*. 2004;7(11):1173-1174.
21. Wallis JD. Cross-species studies of orbitofrontal cortex and value-based decision-making. *Nature neuroscience*. 2012;15(1):13-19.
22. Howard JD, Kahnt T. To be specific: The role of orbitofrontal cortex in signaling reward identity. *Behavioral Neuroscience*. 2021;
23. Levy DJ, Glimcher PW. The root of all value: a neural common currency for choice. *Current opinion in neurobiology*. 2012;22(6):1027-1038.
24. Schoenbaum G, Roesch MR, Stalnaker TA, Takahashi YK. A new perspective on the role of the orbitofrontal cortex in adaptive behaviour. *Nature Reviews Neuroscience*. 2009;10(12):885-892.
25. Schoenbaum G, Takahashi Y, Liu T-L, McDannald MA. Does the orbitofrontal cortex signal value? *Annals of the New York Academy of Sciences*. 2011;1239:87.
26. Wikenheiser AM, Schoenbaum G. Over the river, through the woods: cognitive maps in the hippocampus and orbitofrontal cortex. *Nature Reviews Neuroscience*. 2016;17(8):513-523.
27. Bechara A, Tranel D, Damasio H. Characterization of the decision-making deficit of patients with ventromedial prefrontal cortex lesions. *Brain*. 2000;123(11):2189-2202.

28. Floden D, Alexander MP, Kubu C, Katz D, Stuss DT. Impulsivity and risk-taking behavior in focal frontal lobe lesions. *Neuropsychologia*. 2008;46(1):213-223.
29. Stuss D, Levine B, Alexander M, et al. Wisconsin Card Sorting Test performance in patients with focal frontal and posterior brain damage: effects of lesion location and test structure on separable cognitive processes. *Neuropsychologia*. 2000;38(4):388-402.
30. Gottfried JA, Zelano C. The value of identity: olfactory notes on orbitofrontal cortex function. *Annals of the New York Academy of Sciences*. 2011;1239(1):138-148.
31. McDannald MA, Esber GR, Wegener MA, et al. Orbitofrontal neurons acquire responses to 'valueless' Pavlovian cues during unblocking. *Elife*. 2014;3:e02653.
32. Stalnaker TA, Cooch NK, McDannald MA, Liu T-L, Wied H, Schoenbaum G. Orbitofrontal neurons infer the value and identity of predicted outcomes. *Nature communications*. 2014;5(1):1-13.
33. Schuck NW, Cai MB, Wilson RC, Niv Y. Human orbitofrontal cortex represents a cognitive map of state space. *Neuron*. 2016;91(6):1402-1412.
34. Stalnaker TA, Cooch NK, Schoenbaum G. What the orbitofrontal cortex does not do. *Nature neuroscience*. 2015;18(5):620-627.
35. Wilson RC, Takahashi YK, Schoenbaum G, Niv Y. Orbitofrontal cortex as a cognitive map of task space. *Neuron*. 2014;81(2):267-279.
36. Petrides M. The orbitofrontal cortex: novelty, deviation from expectation, and memory. *Annals of the New York Academy of Sciences*. 2007;1121(1):33-53.
37. Sul JH, Kim H, Huh N, Lee D, Jung MW. Distinct roles of rodent orbitofrontal and medial prefrontal cortex in decision making. *Neuron*. 2010;66(3):449-460.
38. Thorpe S, Rolls E, Maddison S. The orbitofrontal cortex: neuronal activity in the behaving monkey. *Experimental brain research*. 1983;49(1):93-115.
39. Wallis JD, Rich EL. Challenges of interpreting frontal neurons during value-based decision-making. *Frontiers in neuroscience*. 2011;5:124.
40. Nobre A, Coull J, Frith C, Mesulam M. Orbitofrontal cortex is activated during breaches of expectation in tasks of visual attention. *Nature neuroscience*. 1999;2(1):11-12.
41. Schultz W, Dickinson A. Neuronal coding of prediction errors. *Annual review of neuroscience*. 2000;23(1):473-500.
42. Tobler PN, O'Doherty JP, Dolan RJ, Schultz W. Human neural learning depends on reward prediction errors in the blocking paradigm. *Journal of Neurophysiology*. 2006;95(1):301-310.
43. Bar M. Predictions: a universal principle in the operation of the human brain. The Royal Society London; 2009.
44. Clark A. Whatever next? Predictive brains, situated agents, and the future of cognitive science. *Behavioral and brain sciences*. 2013;36(3):181-204.
45. Friston K. The free-energy principle: a unified brain theory? *Nature reviews neuroscience*. 2010;11(2):127-138.
46. Rao RP. Bayesian inference and attentional modulation in the visual cortex. *Neuroreport*. 2005;16(16):1843-1848.
47. Friston K. A theory of cortical responses. *Philosophical transactions of the Royal Society B: Biological sciences*. 2005;360(1456):815-836.
48. Mumford D. On the computational architecture of the neocortex. *Biological cybernetics*. 1992;66(3):241-251.
49. Rao RP, Ballard DH. Predictive coding in the visual cortex: a functional interpretation of some extra-classical receptive-field effects. *Nature neuroscience*. 1999;2(1):79-87.
50. Srinivasan MV, Laughlin SB, Dubs A. Predictive coding: a fresh view of inhibition in the retina. *Proceedings of the Royal Society of London Series B Biological Sciences*. 1982;216(1205):427-459.

51. Chennu S, Noreika V, Gueorguiev D, Shtyrov Y, Bekinschtein TA, Henson R. Silent expectations: dynamic causal modeling of cortical prediction and attention to sounds that weren't. *Journal of Neuroscience*. 2016;36(32):8305-8316.
52. Garrido MI, Friston KJ, Kiebel SJ, Stephan KE, Baldeweg T, Kilner JM. The functional anatomy of the MMN: a DCM study of the roving paradigm. *Neuroimage*. 2008;42(2):936-944.
53. Garrido MI, Kilner JM, Kiebel SJ, Friston KJ. Dynamic causal modeling of the response to frequency deviants. *Journal of Neurophysiology*. 2009;101(5):2620-2631.
54. Phillips HN, Blenkmann A, Hughes LE, Bekinschtein TA, Rowe JB. Hierarchical organization of frontotemporal networks for the prediction of stimuli across multiple dimensions. *Journal of Neuroscience*. 2015;35(25):9255-9264.
55. Phillips HN, Blenkmann A, Hughes LE, Kochen S, Bekinschtein TA, Rowe JB. Convergent evidence for hierarchical prediction networks from human electrocorticography and magnetoencephalography. *cortex*. 2016;82:192-205.
56. Alexander WH, Brown JW. Medial prefrontal cortex as an action-outcome predictor. *Nature neuroscience*. 2011;14(10):1338-1344.
57. Alexander WH, Brown JW. A general role for medial prefrontal cortex in event prediction. *Frontiers in computational neuroscience*. 2014;8:69.
58. Chennu S, Noreika V, Gueorguiev D, et al. Expectation and attention in hierarchical auditory prediction. *Journal of Neuroscience*. 2013;33(27):11194-11205.
59. Doricchi F, Pinto M, Pellegrino M, et al. Deficits of hierarchical predictive coding in left spatial neglect. *Brain communications*. 2021;3(2):fcab111.
60. Garrido MI, Kilner JM, Kiebel SJ, Friston KJ. Evoked brain responses are generated by feedback loops. *Proceedings of the National Academy of Sciences*. 2007;104(52):20961-20966.
61. Lieder F, Daunizeau J, Garrido MI, Friston KJ, Stephan KE. Modelling trial-by-trial changes in the mismatch negativity. *PLoS computational biology*. 2013;9(2):e1002911.
62. Wacongne C, Labyt E, van Wassenhove V, Bekinschtein T, Naccache L, Dehaene S. Evidence for a hierarchy of predictions and prediction errors in human cortex. *Proceedings of the National Academy of Sciences*. 2011;108(51):20754-20759.
63. Hoy CW, Steiner SC, Knight RT. Single-trial modeling separates multiple overlapping prediction errors during reward processing in human EEG. *Communications Biology*. 2021;4(1):1-17.
64. Näätänen R, Gaillard AW, Mäntysalo S. Early selective-attention effect on evoked potential reinterpreted. *Acta psychologica*. 1978;42(4):313-329.
65. Näätänen R, Paavilainen P, Rinne T, Alho K. The mismatch negativity (MMN) in basic research of central auditory processing: a review. *Clinical neurophysiology*. 2007;118(12):2544-2590.
66. Parmentier FB, Elsley JV, Andrés P, Barceló F. Why are auditory novels distracting? Contrasting the roles of novelty, violation of expectation and stimulus change. *Cognition*. 2011;119(3):374-380.
67. Winkler I. Interpreting the mismatch negativity. *Journal of Psychophysiology*. 2007;21(3-4):147-163.
68. Opitz B, Rinne T, Mecklinger A, Von Cramon DY, Schröger E. Differential contribution of frontal and temporal cortices to auditory change detection: fMRI and ERP results. *Neuroimage*. 2002;15(1):167-174.
69. Doeller CF, Opitz B, Mecklinger A, Krick C, Reith W, Schröger E. Prefrontal cortex involvement in preattentive auditory deviance detection:: neuroimaging and electrophysiological evidence. *Neuroimage*. 2003;20(2):1270-1282.

70. Liebenthal E, Ellingson ML, Spanaki MV, Prieto TE, Ropella KM, Binder JR. Simultaneous ERP and fMRI of the auditory cortex in a passive oddball paradigm. *Neuroimage*. 2003;19(4):1395-1404.
71. Molholm S, Martinez A, Ritter W, Javitt DC, Foxe JJ. The neural circuitry of pre-attentive auditory change-detection: an fMRI study of pitch and duration mismatch negativity generators. *Cerebral Cortex*. 2005;15(5):545-551.
72. Shalgi S, Deouell LY. Direct evidence for differential roles of temporal and frontal components of auditory change detection. *Neuropsychologia*. 2007;45(8):1878-1888.
73. Deouell LY. The frontal generator of the mismatch negativity revisited. *Journal of Psychophysiology*. 2007;21(3-4):188-203.
74. Garrido MI, Kilner JM, Stephan KE, Friston KJ. The mismatch negativity: a review of underlying mechanisms. *Clinical neurophysiology*. 2009;120(3):453-463.
75. Nourski KV, Steinschneider M, Rhone AE, Kawasaki H, Howard III MA, Banks MI. Processing of auditory novelty across the cortical hierarchy: An intracranial electrophysiology study. *Neuroimage*. 2018;183:412-424.
76. Nourski KV, Steinschneider M, Rhone AE, Kawasaki H, Howard MA, Banks MI. Auditory predictive coding across awareness states under anesthesia: an intracranial electrophysiology study. *Journal of Neuroscience*. 2018;38(39):8441-8452.
77. Blenkmann AO, Collavini S, Lubell J, et al. Auditory deviance detection in the human insula: An intracranial EEG study. *Cortex*. 2019;121:189-200.
78. Bekinschtein TA, Dehaene S, Rohaut B, Tadel F, Cohen L, Naccache L. Neural signature of the conscious processing of auditory regularities. *Proceedings of the National Academy of Sciences*. 2009;106(5):1672-1677.
79. El Karoui I, King J-R, Sitt J, et al. Event-related potential, time-frequency, and functional connectivity facets of local and global auditory novelty processing: an intracranial study in humans. *Cerebral cortex*. 2015;25(11):4203-4212.
80. Kompus K, Volehaugen V, Todd J, Westerhausen R. Hierarchical modulation of auditory prediction error signaling is independent of attention. *Cognitive neuroscience*. 2020;11(3):132-142.
81. Polich J. Updating P300: an integrative theory of P3a and P3b. *Clinical neurophysiology*. 2007;118(10):2128-2148.
82. Squires NK, Squires KC, Hillyard SA. Two varieties of long-latency positive waves evoked by unpredictable auditory stimuli in man. *Electroencephalography and clinical neurophysiology*. 1975;38(4):387-401.
83. Escera C, Corral M. Role of mismatch negativity and novelty-P3 in involuntary auditory attention. *Journal of psychophysiology*. 2007;21(3-4):251-264.
84. Corbetta M, Shulman GL. Control of goal-directed and stimulus-driven attention in the brain. *Nature reviews neuroscience*. 2002;3(3):201-215.
85. Corbetta M, Patel G, Shulman GL. The reorienting system of the human brain: from environment to theory of mind. *Neuron*. 2008;58(3):306-324.
86. Nieuwenhuis S, Aston-Jones G, Cohen JD. Decision making, the P3, and the locus coeruleus--norepinephrine system. *Psychological bulletin*. 2005;131(4):510.
87. Donchin E, Coles MG. Is the P300 component a manifestation of context updating? *Behavioral and brain sciences*. 1988;11(3):357-374.
88. Chao L, Nielsen-Bohlman L, Knight R. Auditory event-related potentials dissociate early and late memory processes. *Electroencephalography and Clinical Neurophysiology/Evoked Potentials Section*. 1995;96(2):157-168.
89. Picton TW. The P300 wave of the human event-related potential. *Journal of clinical neurophysiology*. 1992;9(4):456-479.

90. Sergent C, Baillet S, Dehaene S. Timing of the brain events underlying access to consciousness during the attentional blink. *Nature neuroscience*. 2005;8(10):1391-1400.
91. Del Cul A, Baillet S, Dehaene S. Brain dynamics underlying the nonlinear threshold for access to consciousness. *PLoS biology*. 2007;5(10):e260.
92. Knight RT. Decreased response to novel stimuli after prefrontal lesions in man. *Electroencephalography and Clinical Neurophysiology/Evoked Potentials Section*. 1984;59(1):9-20.
93. Knight RT, Scabini D. Anatomic bases of event-related potentials and their relationship to novelty detection in humans. *Journal of clinical neurophysiology*. 1998;15(1):3-13.
94. Daffner KR, Mesulam M, Scinto L, et al. The central role of the prefrontal cortex in directing attention to novel events. *Brain*. 2000;123(5):927-939.
95. Daffner KR, Scinto L, Weitzman A, et al. Frontal and parietal components of a cerebral network mediating voluntary attention to novel events. *Journal of cognitive neuroscience*. 2003;15(2):294-313.
96. Soltani M, Knight RT. Neural origins of the P300. *Critical Reviews™ in Neurobiology*. 2000;14(3-4)
97. Kam J, Szczepanski S, Canolty R, et al. Differential sources for 2 neural signatures of target detection: an electrocorticography study. *Cerebral Cortex*. 2018;28(1):9-20.
98. Helfrich RF, Knight RT. Cognitive neurophysiology: event-related potentials. *Handbook of clinical neurology*. 2019;160:543-558.
99. Alho K, Woods DL, Algazi A, Knight R, Näätänen R. Lesions of frontal cortex diminish the auditory mismatch negativity. *Electroencephalography and clinical neurophysiology*. 1994;91(5):353-362.
100. Alain C, Woods DL, Knight RT. A distributed cortical network for auditory sensory memory in humans. *Brain research*. 1998;812(1-2):23-37.
101. Løvstad M, Funderud I, Lindgren M, et al. Contribution of subregions of human frontal cortex to novelty processing. *Journal of cognitive neuroscience*. 2012;24(2):378-395.
102. Solbakk A-K, Lubell J, Leske S, et al. Monitoring of Self-Paced Action Timing and Sensory Outcomes After Lesions to the Orbitofrontal Cortex. *Journal of Cognitive Neuroscience*. 2021:1-20.
103. Wechsler D. Manual for the Wechsler abbreviated intelligence scale (WASI). *San Antonio, TX: The Psychological Corporation*. 1999;
104. Chatrian GE, Lettich E, Nelson PL. Ten percent electrode system for topographic studies of spontaneous and evoked EEG activities. *American Journal of EEG technology*. 1985;25(2):83-92.
105. Oostenveld R, Fries P, Maris E, Schoffelen J-M. FieldTrip: open source software for advanced analysis of MEG, EEG, and invasive electrophysiological data. *Computational intelligence and neuroscience*. 2011;2011
106. Leske S, Dalal SS. Reducing power line noise in EEG and MEG data via spectrum interpolation. *Neuroimage*. 2019;189:763-776.
107. Perrin F, Pernier J, Bertrand O, Echallier JF. Spherical splines for scalp potential and current density mapping. *Electroencephalography and clinical neurophysiology*. 1989;72(2):184-187.
108. Chao ZC, Takaura K, Wang L, Fujii N, Dehaene S. Large-scale cortical networks for hierarchical prediction and prediction error in the primate brain. *Neuron*. 2018;100(5):1252-1266. e3.
109. Maris E, Oostenveld R. Nonparametric statistical testing of EEG-and MEG-data. *Journal of neuroscience methods*. 2007;164(1):177-190.
110. Luck SJ. *An introduction to the event-related potential technique*. MIT press; 2014.

111. Liesefeld HR. Estimating the timing of cognitive operations with MEG/EEG latency measures: a primer, a brief tutorial, and an implementation of various methods. *Frontiers in neuroscience*. 2018;12:765.
112. Sussman ES. A new view on the MMN and attention debate: the role of context in processing auditory events. *Journal of Psychophysiology*. 2007;21(3-4):164-175.
113. Cornella M, Leung S, Grimm S, Escera C. Detection of simple and pattern regularity violations occurs at different levels of the auditory hierarchy. 2012;
114. Strauss M, Sitt JD, King J-R, et al. Disruption of hierarchical predictive coding during sleep. *Proceedings of the National Academy of Sciences*. 2015;112(11):E1353-E1362.
115. Pegado F, Bekinschtein T, Chausson N, Dehaene S, Cohen L, Naccache L. Probing the lifetimes of auditory novelty detection processes. *Neuropsychologia*. 2010;48(10):3145-3154.
116. Polich J, Criado JR. Neuropsychology and neuropharmacology of P3a and P3b. *International Journal of Psychophysiology*. 2006;60(2):172-185.
117. Walentowska W, Moors A, Paul K, Pourtois G. Goal relevance influences performance monitoring at the level of the FRN and P3 components. *Psychophysiology*. 2016;53(7):1020-1033.
118. King J-R, Faugeras F, Gramfort A, et al. Single-trial decoding of auditory novelty responses facilitates the detection of residual consciousness. *Neuroimage*. 2013;83:726-738.
119. Faugeras F, Rohaut B, Weiss N, et al. Event related potentials elicited by violations of auditory regularities in patients with impaired consciousness. *Neuropsychologia*. 2012;50(3):403-418.
120. Faugeras F, Rohaut B, Weiss N, et al. Probing consciousness with event-related potentials in the vegetative state. *Neurology*. 2011;77(3):264-268.
121. Sergent C, Naccache L. Imaging neural signatures of consciousness:‘What’,‘When’,‘Where’and ‘How’does it work? *Archives italiennes de biologie*. 2012;150(2/3):91-106.
122. Aru J, Bachmann T, Singer W, Melloni L. Distilling the neural correlates of consciousness. *Neuroscience & Biobehavioral Reviews*. 2012;36(2):737-746.
123. Baldeweg T. Repetition effects to sounds: evidence for predictive coding in the auditory system. *Trends in cognitive sciences*. 2006;
124. Jemel B, Achenbach C, Müller BW, Röpcke B, Oades RD. Mismatch negativity results from bilateral asymmetric dipole sources in the frontal and temporal lobes. *Brain topography*. 2002;15(1):13-27.
125. Escera C, Alho K, Schröger E, Winkler IW. Involuntary attention and distractibility as evaluated with event-related brain potentials. *Audiology and Neurotology*. 2000;5(3-4):151-166.
126. Escera C, Yago E, Alho K. Electrical responses reveal the temporal dynamics of brain events during involuntary attention switching. *European Journal of Neuroscience*. 2001;14(5):877-883.
127. Friedman D, Cycowicz YM, Gaeta H. The novelty P3: an event-related brain potential (ERP) sign of the brain's evaluation of novelty. *Neuroscience & Biobehavioral Reviews*. 2001;25(4):355-373.
128. Schomaker J, Meeter M. Novelty detection is enhanced when attention is otherwise engaged: an event-related potential study. *Experimental Brain Research*. 2014;232(3):995-1011.
129. Schomaker J, Roos R, Meeter M. Expecting the unexpected: The effects of deviance on novelty processing. *Behavioral Neuroscience*. 2014;128(2):146.
130. Wessel JR, Danielmeier C, Morton JB, Ullsperger M. Surprise and error: common neuronal architecture for the processing of errors and novelty. *Journal of Neuroscience*. 2012;32(22):7528-7537.

131. Wessel JR, Klein TA, Ott DV, Ullsperger M. Lesions to the prefrontal performance-monitoring network disrupt neural processing and adaptive behaviors after both errors and novelty. *Cortex*. 2014;50:45-54.
132. Schomaker J, van Bronkhorst ML, Meeter M. Exploring a novel environment improves motivation and promotes recall of words. *Frontiers in psychology*. 2014;5:918.
133. Schoenbaum G, Roesch M. Orbitofrontal cortex, associative learning, and expectancies. *Neuron*. 2005;47(5):633-636.
134. Schuck NW, Wilson R, Niv Y. A state representation for reinforcement learning and decision-making in the orbitofrontal cortex. *Goal-directed decision making*. Elsevier; 2018:259-278.
135. Niv Y. Learning task-state representations. *Nature neuroscience*. 2019;22(10):1544-1553.
136. Zhou J, Montesinos-Cartagena M, Wikenheiser AM, Gardner MP, Niv Y, Schoenbaum G. Complementary task structure representations in hippocampus and orbitofrontal cortex during an odor sequence task. *Current Biology*. 2019;29(20):3402-3409. e3.
137. Dehaene S, Changeux J-P. Experimental and theoretical approaches to conscious processing. *Neuron*. 2011;70(2):200-227.
138. Wilson B, Marslen-Wilson WD, Petkov CI. Conserved sequence processing in primate frontal cortex. *Trends in neurosciences*. 2017;40(2):72-82.
139. Wilson B, Smith K, Petkov CI. Mixed-complexity artificial grammar learning in humans and macaque monkeys: evaluating learning strategies. *European Journal of Neuroscience*. 2015;41(5):568-578.
140. Uhrig L, Dehaene S, Jarraya B. A hierarchy of responses to auditory regularities in the macaque brain. *Journal of Neuroscience*. 2014;34(4):1127-1132.
141. Wang L, Uhrig L, Jarraya B, Dehaene S. Representation of numerical and sequential patterns in macaque and human brains. *Current Biology*. 2015;25(15):1966-1974.
142. Petrides M, Alivisatos B, Frey S. Differential activation of the human orbital, mid-ventrolateral, and mid-dorsolateral prefrontal cortex during the processing of visual stimuli. *Proceedings of the National Academy of Sciences*. 2002;99(8):5649-5654.
143. Rolls ET, Browning AS, Inoue K, Hernadi I. Novel visual stimuli activate a population of neurons in the primate orbitofrontal cortex. *Neurobiology of learning and memory*. 2005;84(2):111-123.
144. Rolls ET. *The orbitofrontal cortex*. Oxford University Press; 2019.
145. Berlin H, Rolls E, Kischka U. Impulsivity, time perception, emotion and reinforcement sensitivity in patients with orbitofrontal cortex lesions. *Brain*. 2004;127(5):1108-1126.
146. Picton TW, Stuss DT, Shallice T, Alexander MP, Gillingham S. Keeping time: effects of focal frontal lesions. *Neuropsychologia*. 2006;44(7):1195-1209.

A Group overlay of lesion reconstruction

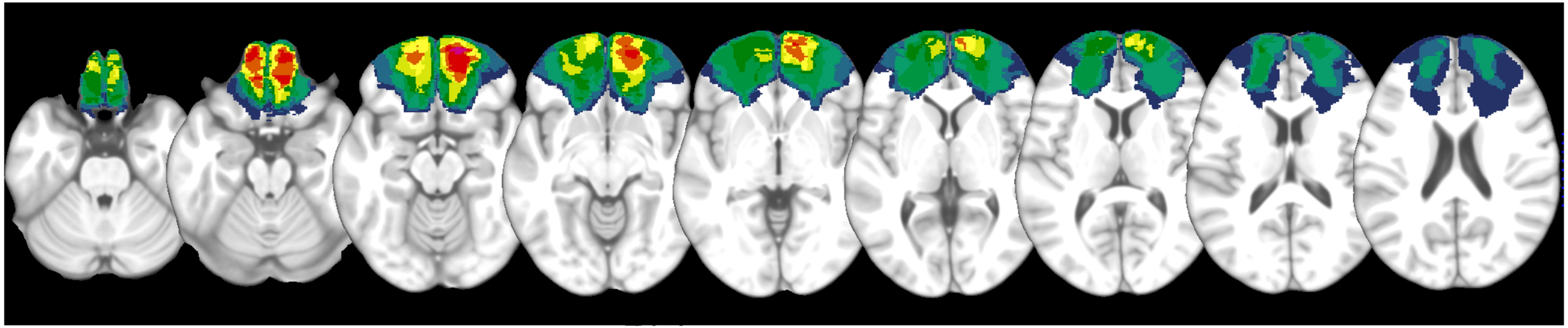

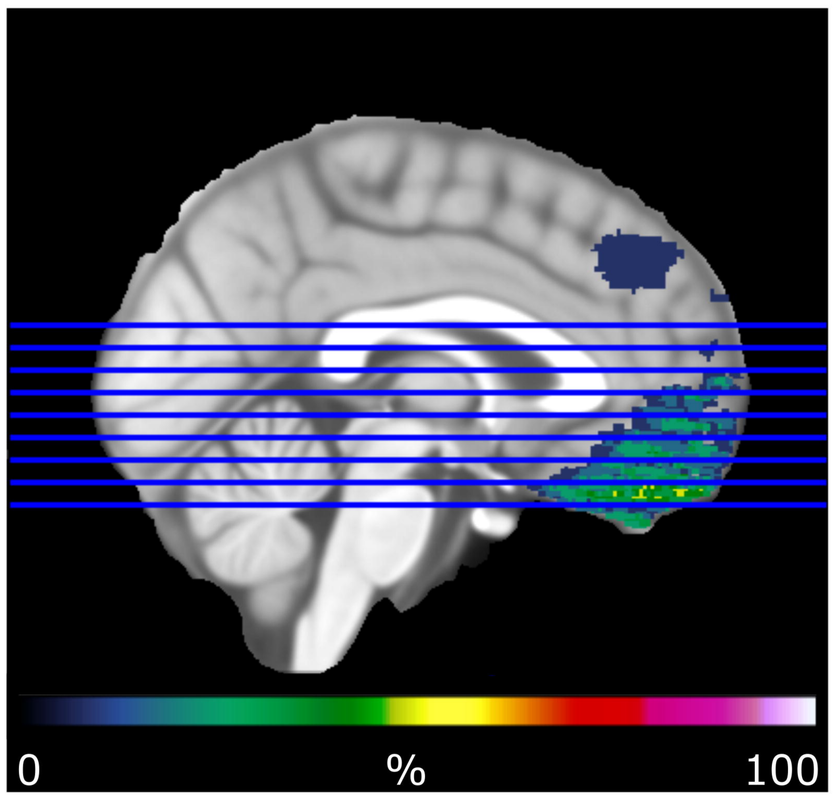

B Lesion by Brodmann Areas

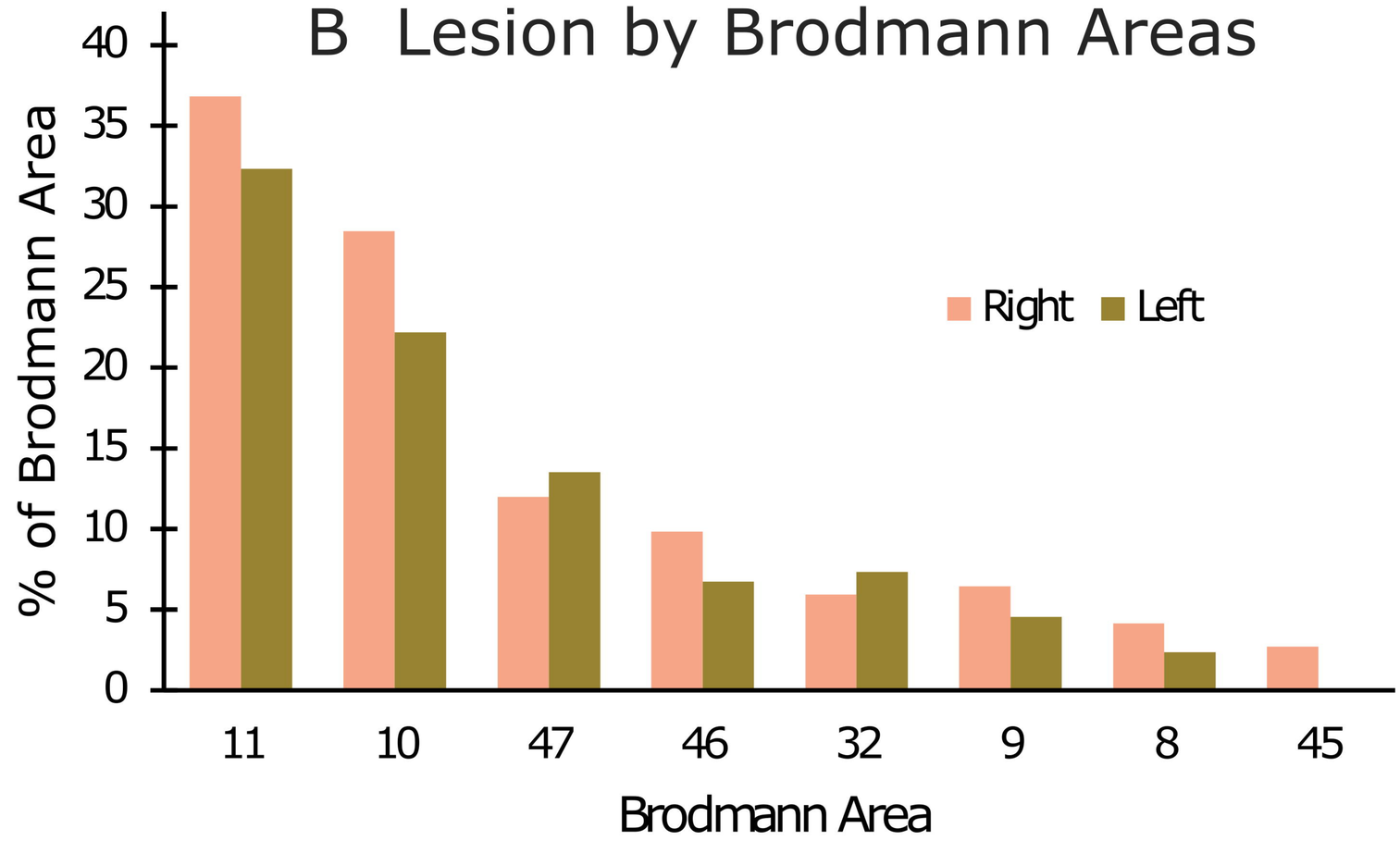

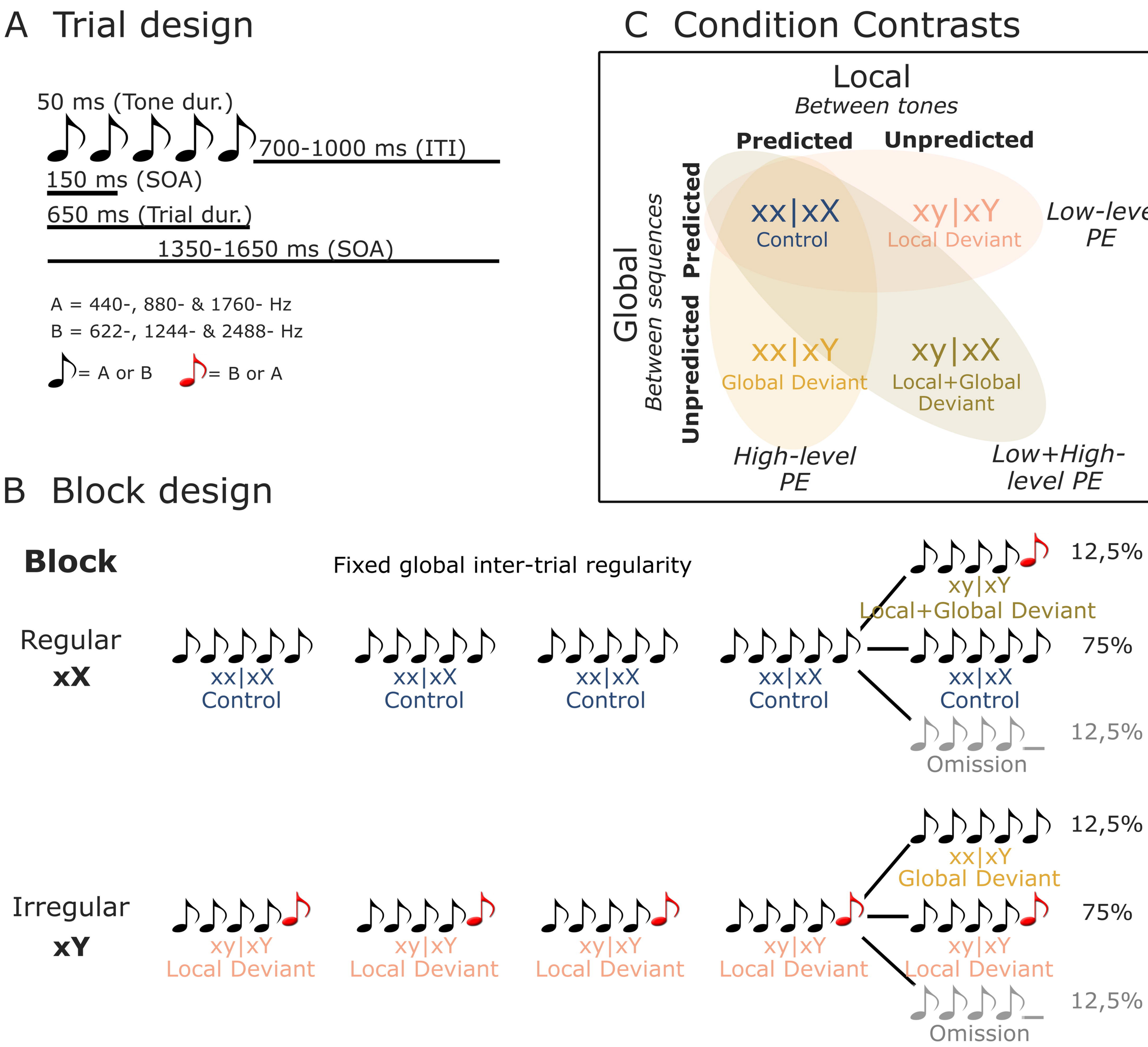
A Trial design
50 ms (Tone dur.)
700-1000 ms (ITI)
150 ms (SOA)
650 ms (Trial dur.)
1350-1650 ms (SOA)
A = 440-, 880- & 1760- Hz
B = 622-, 1244- & 2488- Hz
= A or B
= B or A
C Condition Contrasts
Local
Between tones
Predicted
Unpredicted
Global
Between sequences
Predicted
Unpredicted
xx|xX
Control
xy|xY
Local Deviant
Low-level PE
xx|xY
Global Deviant
xy|xX
Local+Global Deviant
High-level PE
Low+High-level PE
B Block design
Block
Fixed global inter-trial regularity
Regular
xX
xx|xX
Control
12,5%
xy|xY
Local+Global Deviant
75%
Omission
Irregular
xY
xy|xY
Local Deviant
xx|xY
Global Deviant

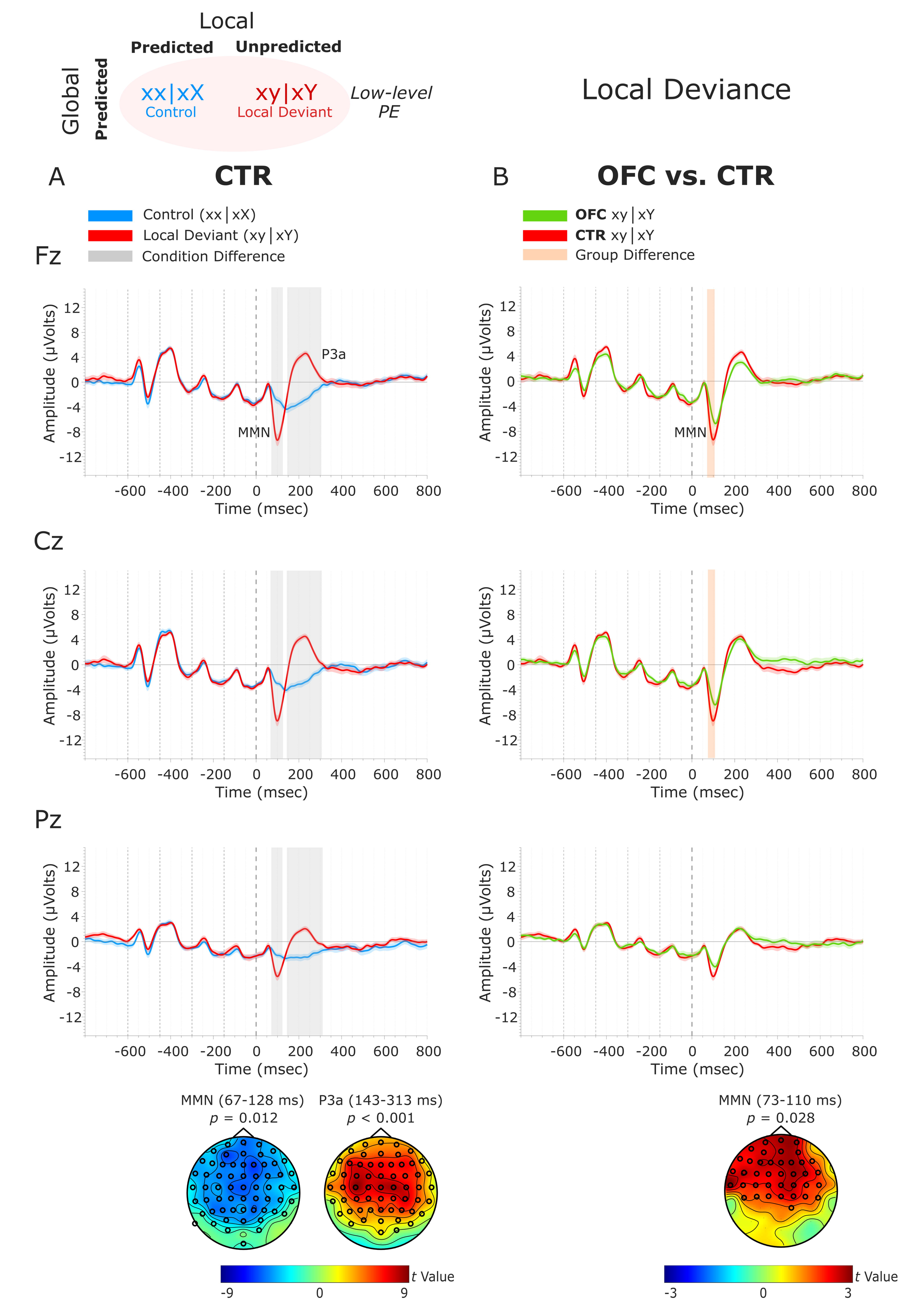
Local
Predicted
Unpredicted
Global
Predicted
xx|xX
Control
xy|xY
Local Deviant
Low-level PE
Local Deviance
A
CTR
B
OFC vs. CTR
Control (xx|xX)
Local Deviant (xy|xY)
Condition Difference
OFC xy|xY
CTR xy|xY
Group Difference
Fz
Cz
Pz
Amplitude (µVolts)
Time (msec)
P3a
MMN
MMN (67-128 ms)
p = 0.012
P3a (143-313 ms)
p < 0.001
MMN (73-110 ms)
p = 0.028
t Value
-9
0
9
-3
0
3

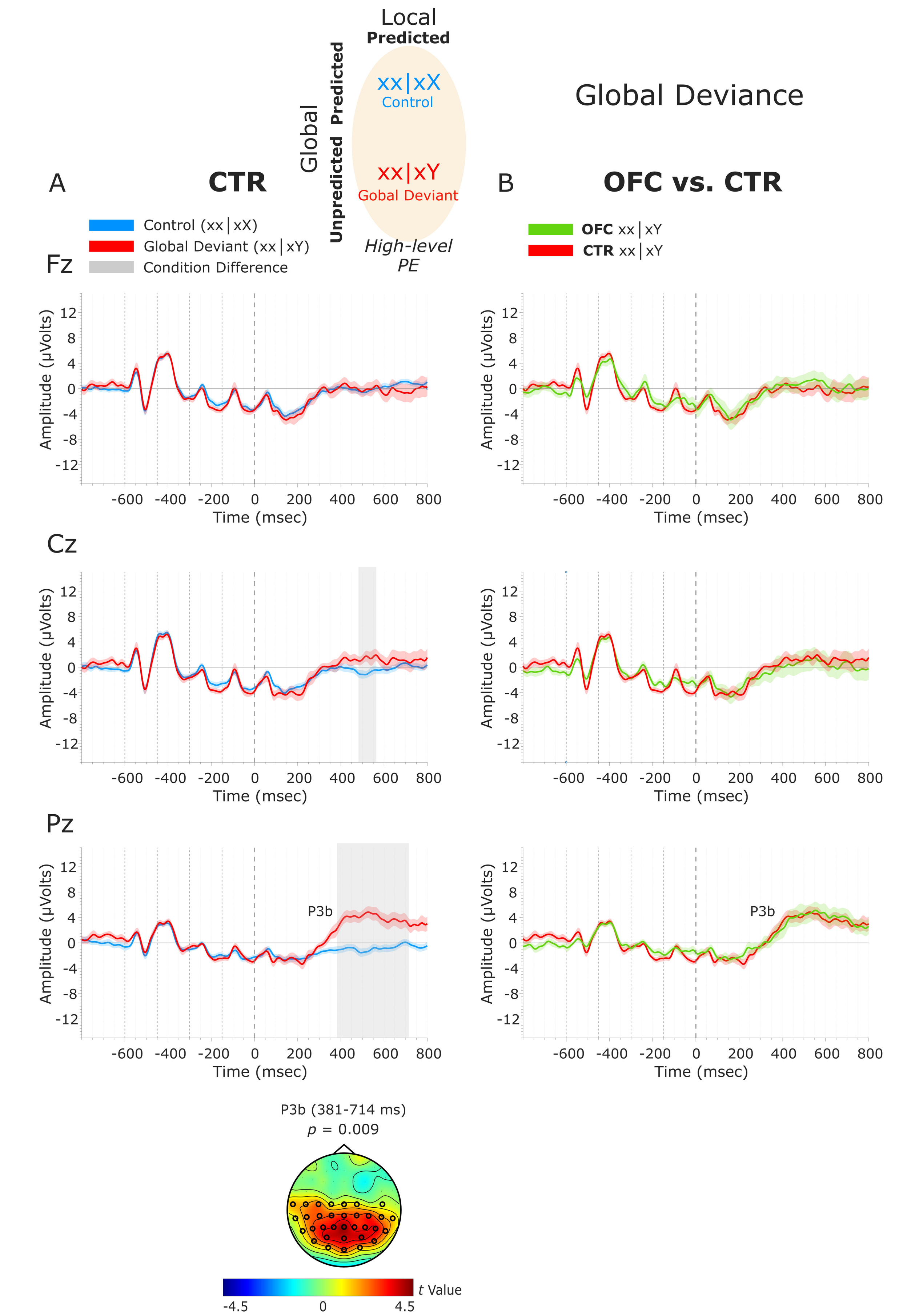
Local
Predicted
Global
Predicted
Unpredicted
xx|xX
Control
xx|xY
Gobal Deviant
High-level PE
Global Deviance
A
CTR
Control (xx|xX)
Global Deviant (xx|xY)
Condition Difference
B
OFC vs. CTR
OFC xx|xY
CTR xx|xY
Fz
Cz
Pz
Amplitude (µVolts)
Time (msec)
P3b
P3b (381-714 ms)
p = 0.009
t Value
-4.5
0
4.5

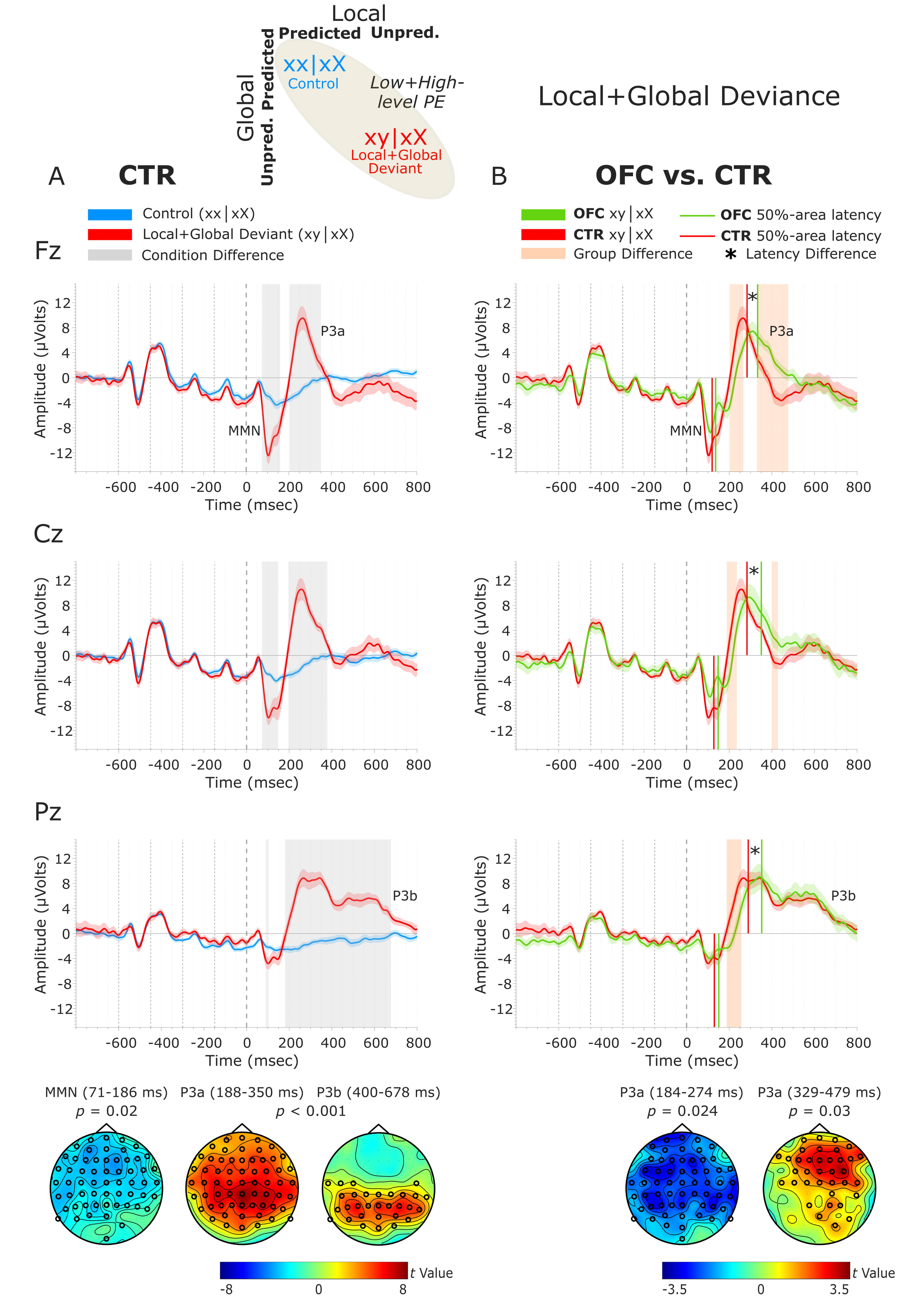
Local
Predicted
Unpred.
Global
Predicted
Unpred.
xx|xX
Control
Low+High-level PE
xy|xX
Local+Global Deviant
Local+Global Deviance
A
CTR
B
OFC vs. CTR
Control (xx|xX)
Local+Global Deviant (xy|xX)
Condition Difference
OFC xy|xX
CTR xy|xX
Group Difference
OFC 50%-area latency
CTR 50%-area latency
Latency Difference
Fz
Cz
Pz
Amplitude (µVolts)
Time (msec)
P3a
MMN
P3b
MMN (71-186 ms)
p = 0.02
P3a (188-350 ms)
P3b (400-678 ms)
p < 0.001
P3a (184-274 ms)
p = 0.024
P3a (329-479 ms)
p = 0.03
t Value
-8
0
8
-3.5
0
3.5